Recent Advances in Flame Retardant and Mechanical Properties of Polylactic Acid: A Review

Xiao-Mei Yang [a, #], Shuang Qiu [b, #], Abdulmalik Yusuf [c], Jun Sun [b, *], Zhongjie Zhai [a],

Junhuan Zhao [a, *], Guang-Zhong Yin [d, *]

[a] *Zhejiang Ruico Advanced Material Co., Ltd., Huzhou 313018, Zhejiang Province, China*
[b] *Beijing University of Chemical Technology, 100029, Beijing, China*
[c]*E.T.S. de Ingenieros de Caminos, Universidad Politécnica de Madrid, C/Profesor Aranguren 3, 28040 Madrid, Spain*
[d]*Escuela Politécnica Superior, Universidad Francisco de Vitoria, Ctra. Pozuelo-Majadahonda Km 1.800, 28223, Pozuelo de Alarcón, Madrid, Spain*
[#] *The authors contributed equally to the work.*
***Corresponding author**: amos.guangzhong@ufv.es (G. Y.), sunj@mail.buct.edu.cn (J. S.), gm@hzruico.com (J. Z.)

Abstract. The large-scale application of ecofriendly polymeric materials has become a key focus of scientific research with the trend toward sustainable development. Mechanical properties and fire safety are two critical considerations of biopolymers for large-scale applications. Polylactic acid (PLA) is a flammable, melt-drop carrying, and strong but brittle polymer. Hence, it is essential to achieve both flame retardancy and mechanical enhancement to improve safety and broaden its application. This study reviews the recent research on the flame retardant functionalization and mechanical reinforcement of PLA. It classifies PLA according to the type of the flame retardant strategy employed, such as surface-modified fibers, modified nano/micro fillers, small-molecule and macromolecular flame retardants, flame retardants with fibers or polymers, and chain extension or crosslinking with other flame retardants. The functionalization strategies and main parameters of the modified PLA systems are summarized and analyzed. This study summarizes the latest advances in the fields of flame retardancy and mechanical reinforcement of PLA.

Keywords: Sustainable polymer; Flame retardant; Biodegradable; Polylactic acid; Nanocomposites

Abbreviations

AHP	Aluminum hypophosphite
APP	Ammonium polyphosphate
ASC	P-amino-benzenersulfonic acid
ATH	Aluminum hypophosphite
ATMP	Trimethylene phosphonic acid
BATDMS	1, 3-bis(3-aminopropyl) tetramethyl-disloxane
BSi	Polyborosiloxane
CCT	CONE Calorimeter test
CNF	Carbon nanofiber
CNM	Carbon nanomaterials
CNT	Carbon nanotube
CS	Chitosan
DETA	Diethylenetriamine
DMMP	Dimethyl methylphosphonate
DOPO	10-Dihydro-9-oxa-10-phosphaphenanthrene10-oxide9
EG	Expandable graphite
ESO	Epoxidized soybean oil
FA	Furfurylamine
FR	Flame retardant
FRI	Flame Retardancy Index
GF	Glass fiber
GMA	Glycidyl methacrylate
GO	Graphite oxide
h-BN	Hexagonal boron nitride
HDA	1,6-hexanediamine
HDI	Hexamethylene diisocyanate
HRR	Heat release rate
ILs	Ionic liquids
KFS	Keratin fibers
LbL	Layer-by-layer assembly

LDH	Layered double hydroxide
LOI	Limited oxygen index
MA	Maleic anhydride
MCA	Melamine cyanurate
MDI	4,40-methylenediphenyl diisocyanate
MMT	Montmorillonite
MOF	Metal-organic framework
NA	Nicotinamide
NR	Natural rubber
ODA	4,4’-diaminodiphenyl ether
OPS	Polyhedral octaphenyl silsesquioxane
RA	Reinforcing agent
RGO	Reduced graphene oxide
ROP	Ring-opening polymerization
PA	Phytic acid
PBAT	Polybutylene adipate terephthalate
PBS	Poly(butylene succinate)
PC	Biopolyelectrolyte
PCL	Poly(ε-caprolactone)
PDA	Polydopamine
PEG	Polyethylene glycol
PEI	Polyethylenimine
PHA	Poly(hydroxybutyrate)
pHRR	Peak of heat release
PLA	Polylactic acid
POC	Phosphorus oxychloride
POSS	Polyhedral oligomeric silsesquioxanes
PPA	Phenylphosphinic acid
PPC	Poly(propyl carbonate)
PPDAs	Polyphosphoramides
PPDC	Phenylphosphonic dichloride

PPDCl	Phenylphosphoryl dichloride
PVA	Polyvinyl alcohol
TA	Tannic acid
TCP	Tricresyl phosphate
TDI	Toluenediphenyl diisocyanate
TEC	Triethyl citrate
TGIC	Triglycidyl isocyanurate
THR	Total heat release
TSR	Total smoke emission
TP	Triphenyl phosphate
TTI	Time to Ignition
VOCs	Volatile organic compounds
WF	Wool fiber

1. Introduction

The rapid accumulation of polymer waste in the environment has drawn increasing attention to the use of ecofriendly alternatives in the ever-growing area of polymer applications. Unlike conventional petroleum-based polymers, biodegradable polymers can mitigate environmental threats, facilitating their rapid growth as promising alternatives to wood, metal, and glass. Polylactic acid (PLA), a linear polyester, can be obtained entirely from renewable resources like corn, sugar, or potatoes. Biodegradability, mechanical strength, transparency, and composability are some of the excellent properties of the polymer. PLA degrades to small molecules, such as carbon dioxide, water, and methane, within a few months or a year, presenting a distinct advantage over other polymers with prolonged degradation time under normal environmental conditions [1, 2]. **Figure 1a** shows the increasing publications on PLA over the past 10 y. Approximately 47% of the analytical studies are on PLA plastics, whereas 34% and 9% of studies are on PLA films and gels, respectively.

PLA, a bio-based degradable polymer, is inherently flammable with a limited oxygen index of 18%–20% [3]. It burns with a clean blue flame and carries highly mobile molten droplets but does not produce corrosive or toxic gases. This has caused serious safety hazards in PLA applications, such as packaging, textiles, electrical appliances, and electronic equipment. Therefore, flame-retardancy standards should be achieved prior to PLA’s wide applications as a substitute for nonbiodegradable materials. The high production cost of PLA further restricts its large-scale industrialization. The addition of fillers to PLA reduces the production cost and enhances its durability, impact resistance, tensile strength [4], operation temperature [5], and long-term stability [2]. Several studies have investigated PLA properties with different flame retardants (FRs) and fillers to improve their flame retardancy and mechanical properties, as shown in **Figure 1b**. The literature on FR and reinforced PLA has shown rapid growth since 2010. Compared to the studies focusing on the mechanical reinforcement of PLA, those focusing on the FR properties of PLA have shown an increasing trend annually.

Unlike conventional polymers, biodegradable polymers are more polar, good absorbents, and reactive under ambient conditions. Thus, it is difficult to perform thermal processes, control their mechanical properties, and identify suitable FRs to combine during their decomposition stages. Halogen-based FRs are widely used to enhance FR properties [6, 7]. However, brominated dibenzo-p-dioxins and dibenzofurans are toxic and corrosive gases, limiting their applications according to international treaties [8, 9]. An effective approach for PLA, a polyester polymer, is to promote the formation of insulating carbon layers during combustion to replace the halogen-based FRs [10]. Hence, metal oxides, phosphorus/nitrogen FRs (P–N FRs) [11], nano-FRs [12], bio-based FRs [13,14], and other environmentally friendly additives have been designed in recent years. These alternative ecofriendly FR additives are multifunctional and simultaneously enhance the mechanical performance of the matrix.

Considering the increasing trend of FR applications of bio-based polymers, particularly PLA, this study aims to summarize the recent progress of PLA-based FR reinforcements with a perspective for future trends. Two related research reports and reviews have been published. The reports revealed the hazards of the misuse of organohalogen FRs and highlighted environmentally sustainable FRs that are investigated in PLA, such as metal oxides, phosphorus (P)-based systems, nanomaterials, hyperbranched polymers, and their combinations [15]. Yiga et al. reviewed the latest progress in the flame retardancy and thermal stability of agricultural fiber-reinforced PLA over the past decade. Moreover, they proposed feasible schemes and prospects for developing environmentally friendly and PLA-reinforced FRs [16]. This study discusses solutions to two significant constraints (FR modification and mechanical reinforcement) of PLA-based materials based on the latest research progress. By analyzing the successful cases and the common features of results, this study has been designed to form a cognitive system for a green polymer-based FR reinforcement and master the latest relevant developments. Accounting for previous research and ideas, some expectations and prospects for the future development of the green PLA polymer are proposed.

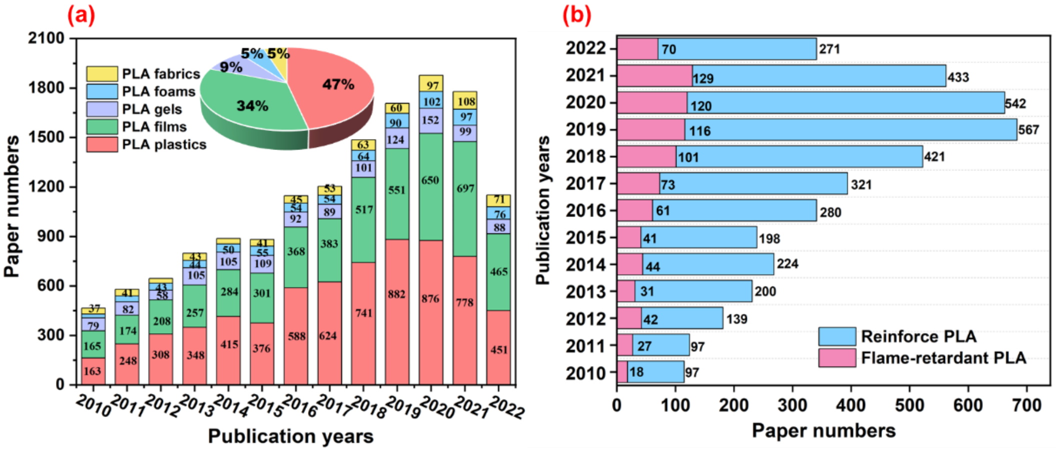

Figure 1. (a) The research on varied PLA products in the past decade and (b) the trend of research on flame-retardant PLA and reinforcing PLA (data from Web of Science, as of September 2022)

2. Flame retardant and reinforcement of polylactic acid

2.1 Flame retardant polylactic acid

PLA, a promising bioplastic, is notable owing to its nontoxicity, high mechanical strength, ease of processing, good biodegradability, and biocompatibility. However, the thermal stability and impact resistance of PLA are inferior to those of the conventional thermoplastic polymers. PLA is flammable, and its combustion is accompanied by molten fluid. Thus, it cannot obtain any rating in the UL-94 vertical burning test. The addition of multifunctional modifiers to PLA is an ideal method of promoting the application of FR PLA in electronics, construction, and automotive industries, and prototyping 3D printing [17, 18]. Substantial progress has been made in this field in recent decades. The addition of specially designed FR additives or fillers with appropriate molecular structures to the matrix imparts high flame retardancy, high mechanical strength, and toughness to polymers. Thus, the flame retardancy and mechanical reinforcement of polymers can be improved [19, 20].

2.2 Reinforcement of polylactic acid

Composites consist of two components: a matrix and a reinforcing material. They are connected through an interface that can retain their original properties and produce synergistic effects after combination to exhibit excellent characteristics that cannot be obtained with a single material. Composites with high-performance fibers as the reinforcing phase and polymers as the matrix have received high attention. High-performance fibers (carbon, glass, and natural fibers) are lightweight and have high specific strengths [21, 22]. They ensure excellent mechanical properties as reinforcements by reducing the density of composites and enabling their applications in aerospace components and lightweight automotive parts [23]. Mechanical properties are fundamental to the practical application of PLA-based materials. Research on the mechanical reinforcement of polymer composites includes material selection, structural design, interface bonding, molding processes, mechanical calculations, and simulations. The mechanical properties of composites can be significantly improved through the structural design of the polymer matrix, surface modification, and the optimization of the molding process.

The preparation of fiber-reinforced composites is divided into two stages. The first stage is the prepreg stage. The polymer is mixed with fibers in the form of a melt, powder, solution, fiber, or film to form a prepreg. The second stage involves the molding of the composite. The prepreg is cut to an appropriate size and placed in a mold following a specific laying sequence. Further impregnation is performed under certain molding conditions, such as temperature and pressure, to obtain a composite with a uniform structure, good interface bonding, and a specific shape. Other methods to strengthen and toughen the PLA matrix of composites include small organic molecules [24], polymeric reinforcements [25], and nanoparticles [26].

3. Practical case for reinforced and flame-retardant polylactic acid

There are many reviews on the FR or reinforcement modification of PLA [16, 27]. This study focuses on a detailed comparative analysis of different categories of modifiers: (1) surface-modified fibers, (2) modified nano/microfillers, (3) small-molecule FRs, (4) macromolecular FRs, (5) FRs with fibers or other polymers, and (6) chain extension or crosslinking with other FRs.

3.1 Surface-modified fibers

Reinforced plastic composites consist of high-modulus fibers (natural and inorganic fibers) that are added to the matrix to avoid various defects such as low melt strength, brittle texture, and poor toughness of polymers. This reinforcement is expected to generate PLA-based composites with excellent performances. The fibers adopted to reinforce PLA composites include natural, synthetic, and inorganic fibers [28, 29]. Fiber-reinforced matrices employ biomass fibers for environmental protection. Sisal, jute, flax, hemp, and wood fibers are different natural fibers used to prepare fully degradable biocomposites at low cost. PLA/natural fiber biocomposites are becoming increasingly popular owing to their renewability and degradability. For the bio-based natural fiber-reinforced PLA, please see other reviews on this topic [30].

The mechanical properties of fiber-reinforced composites are significantly dependent on the intrinsic characteristics of the polymer matrix and natural fibers, and on their interfacial properties [31, 32]. Two methods are mainly applied to improve the compatibility between polymer matrices and fibers: the direct modification of the fiber surface and chemical treatment. Chemical treatment strategies include alkaline, silane, acetylation, benzoylation, peroxide, maleated coupling agents, acrylation, acrylonitrile grafting, isocyanate, permanganate, and fungal treatment [33]. Mixing cellulose fibers with water/acetone and extruding them with PLA improves the Young's modulus and tensile strength of the matrix [34]. Surface-functionalized cellulose nanofibrils obtained via treatment with amines and organic solvents such as acetone or toluene increase the crystallinity and tensile strength of PLA [35, 36].

Current research states that the fiber surface is normally modified by introducing functional components: phosphorus/nitrogen (P–N)-containing compounds, silane coupling agents, and metal complexes to enhance flame retardancy and improve the mechanical properties of biopolymer matrices simultaneously. Yang et al. designed a lignin-derived multifunctional additive (TP-g-lignin) by grafting a P–N-containing vinyl monomer (TP) to lignin. The fibers were immersed in a chemical solution with different FR concentrations. PLA was acceptable with a desirable V-0 rating in the UL-94 test with the incorporation of 5.0 wt% of TP-g-lignin, and the elastic modulus of PLA increased by 26% [37]. A summary of some reported surface modification routes of PLA using fibers is presented in **Figure 2**. The mechanical properties and FR performance results are summarized in **Table 1**.

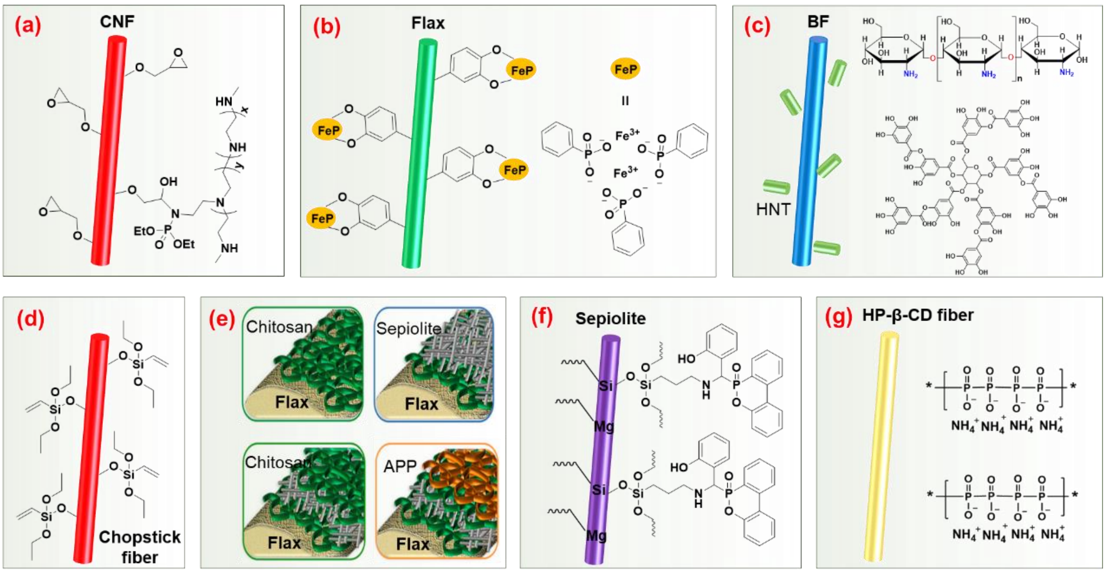

Figure 2. Schematic illustration of (a) the synthetic route of core−shell nanofibrous flame retardants, P/N-FR@CNF (redrawn from reference [38]; copyright (2017) ACS), (b) surface modification of flax fiber by PDA and FeP (redrawn from reference [39]; copyright (2018) Elsevier), (c) the preparation of the flame-retardant BF/PLA mixture (redrawn from reference [40]; copyright (2020) Wiley), (d) reactions of the chopstick fiber with a silane coupling agent (redrawn from reference [41]; copyright (2016) Elsevier), (e) the layer-by-layer assembly and biocomposite preparation procedures (redrawn from reference [42]; copyright (2020) Elsevier), (f) the synthesized SEP-DOPO (SEP as fibrous sepiolite) (redrawn from reference [43]; copyright (2019) Elsevier), and (g) the preparation of the flame-retardant APP/HP-β-CD fiber (redrawn from reference [44]; copyright (2021) Elsevier).

Plant-based fibers are abundant and inexpensive and have high moduli. Plant-based fiber-reinforced PLAs can reduce costs while retaining their biodegradable properties. The surface activity of plant fibers can be improved by alkali treatment, the addition of coupling agents, or by enhancing the interfacial compatibility between PLA and plant fibers with compatibilizers. Cellulose nanofibers (CNF) isolated from plants are considered one of the most promising reinforcing agents for polymers owing to their outstanding mechanical strength and specific surface areas. Feng et al. synthesized a novel high-performance nanofibrous FR by the in-situ chemical grafting of an FR shell onto the CNF surface, as shown in **Figure 2a**. The peak heat release rate (pHRR) of PLA was reduced by 31% with the addition of 10 wt% P–N-FR@CNF, enabling PLA to achieve a UL-94 V-0 rating while increasing the tensile strength and elastic modulus by 24% and 12%, respectively [38]. Flax, one of the earliest natural fibers used by humans, is used as the FR modifier of PLA and reinforces it mechanically. **Figure 2b** shows that raw flax fibers were coated with a polydopamine film in an aqueous solution and ferric phosphonate (FeP) was grown in situ on the fiber surface. The addition of surface-modified flax fibers to PLA increased the limited oxygen index (LOI) from 19.1% to 26.1% and reduced the pHRR by 16% in a CONE Calorimeter test. The modulus increased by 28% to 3594 MPa for FeP-flax/PLA owing to better stress transfer within fiber-reinforced composites [39]. Jin et al. used chitosan (CS) and tannic acid (TA) as cationic and anionic polyelectrolytes, respectively, to modify the surface of bamboo fibers and stabilize halloysite nanotubes (HNT) (**Figure 2c**). The introduction of 5% HNT into bamboo/PLA composites (BPC)/5FR increased the modulus of rupture and modulus of elasticity values by approximately 18.2% and 34.6%, respectively, and the LOI value was increased from 19.1% to 22.5%. Moreover, the total heat release (THR) of the BPC/5FR/HNT also decreased by 17.1% [40]. Wang et al. selected silane coupling agents as compatibilizers to enhance the compatibility between fibers and the matrix. The modified chopstick fibers and nanoclays were grafted onto PLA side chains with reduced agglomeration. Ammonium polyphosphate (APP) and expandable graphite (EG) were also used as FRs in PLA. The final composite tensile and impact strength increments reached 14.5% and

5.5%, respectively. PLA composites achieved a UL-94 V-0 rating when additive loading reached 10 phr of EG or 4 phr APP (**Figure 2d**) [41].

Since its initial use in 1966, the layer-by-layer (LbL) assembly method has been used for the preparation of microspheres and the surface modification of materials [45, 46]. **Figure 2e** shows an LbL technique to modify the surface of flax fabrics by designing as a quad-layer architecture (QL) prior to the PLA combination. The 2.5 QL improved the LOI value of the as-prepared composites to 25.3% with a 33% decrease in the pHRR. The maximum average rate of heat emission was reduced by 30%. The final composite was much stiffer than neat PLA, as demonstrated by a 78% increase in the flexural modulus [42].

Protein-based fibers, derived from animal hair and mineral fibers, play essential roles in PLA reinforcement. Sepiolite (SEP), a natural, nontoxic, and nonradioactive hydrated magnesium silicate clay mineral, was utilized by Jiang et al. as a reinforcing template with its surface grafted with 9,10-dihydro-9-oxy-10-phosphaphenanthrene-10-oxide (DOPO) by condensation between amino groups and salicylaldehyde to obtain DOPO-modified sepiolite (SEP-DOPO) **(Figure 2f)**. The synergistic effect between DOPO and SEP enhanced the formation of the crosslinked structures Si–O–Si, H_3PO_3, and P–N in the condensed-phase carbon. The reinforced PLA exhibited an LOI of 31.5% and achieved a UL-94 V-0 rating with only a 10 wt% loading of SEP-DOPO. Moreover, the pHRR of PLA was reduced by 40.7% [43].

β-cyclodextrin (β-CD) is regarded as an effective carbonizing agent in PLA because of its charge-forming ability and thermal stability. Kata et al. prepared 2-hydroxypropyl-β-cyclodextrin (HP–β-CD) fibers using an aqueous solution-based high-speed electrospinning technique using β-CD as the raw material **(Figure 2g)**. The fibers were added to PLA and APP to obtain the FR composites. The unique microfibrous structure of the oligosaccharide-type carbonizing agent effectively interacted with APP to deliver a good FR effect. The pHRR and THR of PLA/APP/HP-β-CD fibers were decreased by 39.2% and 24.1% than that of pure PLA. The modified fibers exhibited a high LOI value of 32.5%. In contrast, the mechanical properties of PLA composites were negatively affected; the tensile strength and elongation at yield values were reduced by 39.7% and 18.5%, respectively, than those of pure PLA [44].

Table 1. Typical flame retardant and mechanical property parameters of surface-modified fiber-reinforced PLA composites.

Year	**Fillers**	**Types and mechanisms of FRs**	**Impact strength (GPa)**	**Young's modulus (GPa)**	**Elongation at break (%)**	**Tensile Strength (MPa)**	**pHRR (kW/m^2)**	**THR (MJ/m^2)**	**UL-94**	**LOI (%)**	**TTI**	**FRI**	**Rank#**	**Ref**
2017	15% PN-FR@CNF	C-based& P–N-based (C/G case)^	-5.5% (7.2) *****	+26.0% (3.1)	-21.2% (6.3)	+21.2% (70.3)	-31.0%	-12.3%	V0	-	65(69)	1.8	Good; P	[38]
2018	Ferric phosphonate modified flax fiber	P-based &bio-based (C/G case)	-	+34.9% (2.9)	-	-6.3% (55.4)	-16.0%	-2.5%	V2	26.1	47(67)	0.8	Poor; P	[39]
2020	5 wt% HNT+ 5 wt% CS and TA modified the BF	Mineral & bio-based (C/G case)	-	-	-	-	-30.4%, -18.2%	-17.1%	-	22.5	-	-	-;-	[40]
2016	23 phr EG+4 phr APP+25 phr MCF+5 phr MMT	Mineral & P–Si-based (C/G case)	+5.5% (46.4 J/m)	+9.3% (3.5)	-	+14.5% (44.5)	-	-	V0	-	-	-	-; P	[41]
2020	FR coated flax fabrics	P-based & bio-based (C/G case)	-44.0%	+78.0%	-	-	-33.0%	+46.7%	-	25.3	33(48)	1.2	Good; P	[42]
2019	10% SEP-DOPO	P-based & mineral (C/G case)	-	-	-	-	-40.7%	-	V0	31.5	39(38)	1.1	Good; -	[43]
2021	3% HP-β-CD fiber+ 15% APP	P-based & bio-based (C/G case)	-	+1.5% (3.2)	-18.5% (2.2)	-39.7% (36.8)	-39.2%	-24.1%	V2	32.5	45(38)	2.6	Good; N	[44]

Note: + indicates increasing and – indicates decreasing, ^The flame retardant mechanism exerted by FRs is represented by the C case (the condensed phase flame retardant mechanism) and the G case (the gas phase flame retardant mechanism), * the values in brackets are the specific performance data of the modified PLA material, cellulose nanofiber (CNF), diethyl phosphite complexed with polyethyleneimine (PEI) (PN-FR), chitosan (CS), tannic acid (TA), bamboo fiber (BF), halloysite nanotubes (HNT), silane-modified cellulose fiber (MCF), montmorillonite (MMT), expandable graphite (EG), sepiolite (SEP), and β-cyclodextrin (β-CD), #The “Poor,” “Good,” or “Excellent” ranks are assessed for the cases based on the FRI results; P and N indicate the positive and negative effects of flame retardants on the mechanical properties of PLA composites, respectively.

3.2 Nano/micro fillers

Considering the poor flame retardancy of most biocomposites, environmentally sustainable FRs are preferred for improving the fire resistance of PLA while maintaining its biodegradability [10]. Additive-type FRs used in PLA are classified into halogen-, phosphorus-, silicon-, intumescent, inorganic nanomaterials, and bio-based FRs [47, 48]. However, most FRs are ineffective when used separately; therefore, they need to be combined with other additives as synergists. The addition of more than 10 wt% additives result in a decline of mechanical properties affecting its practical applications. In the following sections, we summarize the recent modifications of FRs by physical or chemical methods to obtain good dispersibility, high efficiency, and balanced performance.

3.2.1. Functionalized ammonium polyphosphates

APP, a commonly used P–N FR, is cheap, produces less smoke, is less toxic, and exhibits low corrosion. APP catalyzes the dehydration of the polymer terminal chain and triggers char formation as the FR mechanism. The active radicals (PO_2•, PO•, and HPO•) formed by the P-based compounds volatilize to the gas phase and rapidly scavenge H• and OH• radicals. Since the FR of APP is poor in PLA, it requires a high dosage of APP (15–30 wt%) [49, 50]. APP is normally combined with other additives owing to its low efficiency to promote its char-forming ability through esterification and crosslinking reactions. It is used for surface modification to reduce surface polarity and water solubility, thereby reducing substrate exudation and improving compatibility with organic polymers. Common modification methods include microcapsule coating, coupling-agent blocking, and organic amine ion exchange. This section presents the representative research results of APP surface modification. The relevant mechanical and FR performance indices are listed in **Table 2**, and the illustrated structures are shown in **Figure 3**.

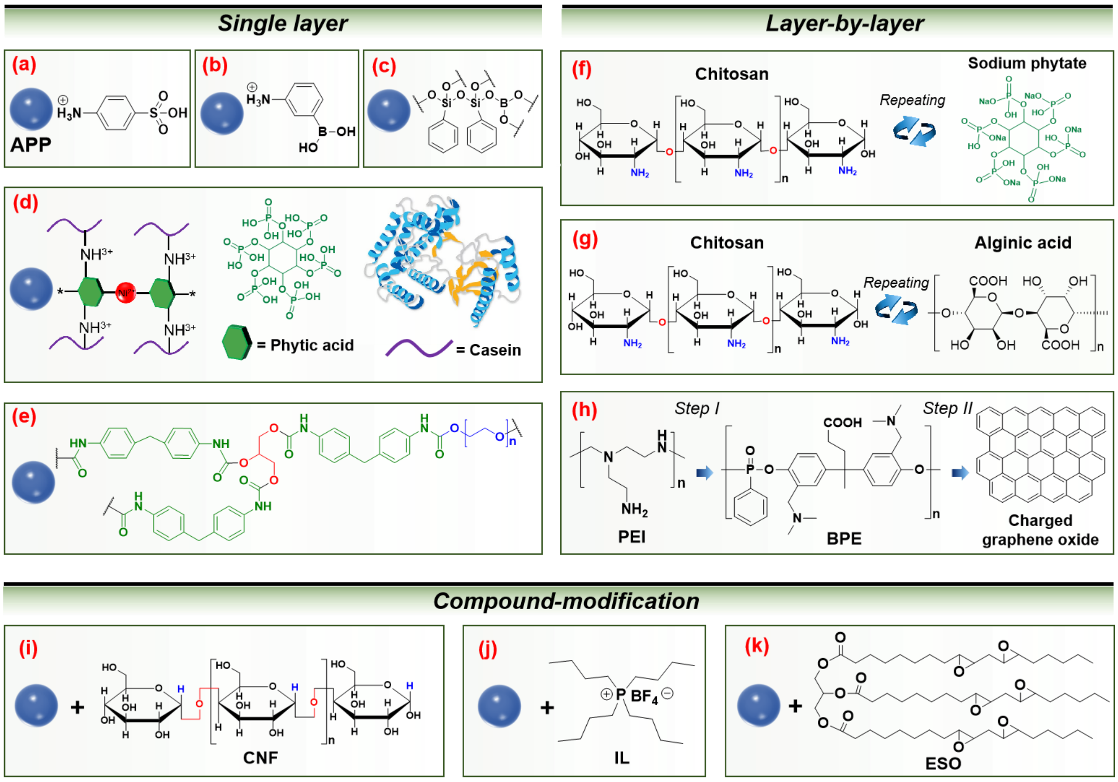

Figure 3. The simplified schematic diagram of the preparation process of (a) A-A [51]; (b) boron-APP [52]; (c) BSi-APP [53]; (d) PC@APP (redrawn from reference [54]; copyright (2019) Elsevier); (e) functional APP (redrawn from reference [55]; copyright (2021) Elsevier); (f) APP@CS@PA-Na via LbL assembly (redrawn from reference [45]; copyright (2019) ACS); (g) APP@CS@AA-nBL (redrawn from reference [56]; copyright (2020) ACS); (h) graphene oxide hybrid (GOH) fabrication via the LbL method (redrawn from reference [57]; copyright (2018) Elsevier); (i) the APP@CNF complex structure based on hydrogen bonding (redrawn from reference [58]; copyright (2018) ACS); (j) the toughening modification of APP blending by ionic liquids (redrawn from reference [47]; copyright (2020) Elsevier), and (k) crosslinked

compound product of epoxidized soybean oil (ESO) and APP (redrawn from reference [59]; copyright (2020) Elsevier).

i. Single-layer chemical surface modification

Piperazine, aminoglycerol, ethanolamine, allylamine, vinyltrimethoxysilane, and various amine compounds have been chemically incorporated into APP via ion-exchange reactions for surface modification [60, 61]. Jin et al. prepared an intumescent FR (IFR) A–A through an ion-exchange reaction between *p*-amino benzenersulfonic acid (ASC) and APP **(Figure 3a)**. As indicated in their study, PLA/15A-A exhibited an increased LOI value of 30.5% with a UL-94 V-0 rating and a lower pHRR (−39.4%) and THR (−27.7%) as compared to those of pristine PLA. Furthermore, ASC introduced organic groups to APP that improved the A–A compatibility in the PLA matrix. The toughness of PLA/15A–A samples increased from 6.9% of pure PLA to 8.0% [51]. Wu et al. reported a method for preparing boron-containing APP (B-APP) via an ion-exchange reaction between 3-aminophenyl boronic acid and APP **(Figure 3b)**. PLA-5% B-APP exhibited a high LOI of 29.4% and showed an acceptable UL-94 V-0 rating. The study also reported improved elongation at break and impact strength of the final composites [52]. The microencapsulation mechanism of APP includes in-situ polymerization, interfacial polymerization, and other reactions. The APP surface is coated with a dense layer of melamine resin, epoxy resin, polyurea, and other shell materials. The compatibility of APP with the polymer is consequently improved under the protection of the microencapsulated shell layer. Therefore, the precipitation of the FR from the polymer is prevented effectively. Ran et al. microencapsulated APP with polyborosiloxane (BSi) to obtain a BSi-APP composite (**Figure 3c**). PLA/5% BSi-APP achieved an LOI value of 26.7% with an acceptable UL-94 V-0 rating.

The microencapsulation of APP improved the compatibility of APP and PLA and the mechanical properties of PLA/5% BSi-APP than those of pristine APP [53]. This team proposed the synthesis of a novel FR with a core–shell structure by combining polyelectrolyte and microcapsule technologies. Phytic acid (PA) reacted with casein (CS) to form a biopolyelectrolyte (PC) and microencapsulated APP as a shell material to obtain PC@APP (**Figure 3d**). Thus, the dispersion of PC@APP in the matrix was significantly enhanced. PLA containing 5% PC@APP improved the elongation at break and notched the impact strength at 6.9% and 3.5 KJ/m^2 compared to neat PLA, which exhibited the same at 14.4% and 4.7 KJ/m^2, respectively. PLA/5% PC@APP showed excellent fire resistance [54]. Zhao et al. prepared a biomimetic peanut leaf structure by directly grafting polymer chains onto the surface of APP to enhance the interfacial adhesion between APP and PLA. The addition of 5 wt% of the newly functionalized melamine polyphosphate imparted good flame retardancy to the material and also increased the elongation at break and the notched Izod impact strength by 21 and 3 times, respectively, compared to those of pure PLA (**Figure 3e**) [55].

ii. Layer-by-Layer assemblies

LbL assemblies were used to construct multilayer core–shell FRs containing APP and polyelectrolytes. The modified PLA samples exhibited enhanced flame retardancy. Xiong et al. demonstrated a green, facile fabrication approach for a core–shell-structured bio-based FR (APP@CS@PA-Na) via LbL assembly in water (**Figure 3f**). The addition of 10 wt% APP@CS@PA-Na allowed the PLA composite to pass the UL-94 V-0 rating. It showed excellent roughness with an increased elongation at the break of 28.4% [45]. Subsequently, this team prepared core–shell FRs (APP@CS@AA-nBL) by self-assembly with APP as the core and a CS/alginate (AA) bilayer as the shell. 10 wt% APP@CS@AA-3BL endowed PLA with a high LOI value of 30.6%, and 23% and 11% reductions of the pHRR and THR, respectively. The impact strength and elongation at break of PLA/10 wt% APP@CS@AA-3BL were improved by 23% and 20.9%, respectively, than those of pure PLA **(Figure 3g**) [56]. A core–shell FR (GOH) was prepared by sequentially depositing polyethyleneimine (PEI), a bio-based polyelectrolyte (BPE), and graphene oxide (pGO) on the surface of APP through electrostatic interactions in an aqueous solution. The introduction of pGO further improved the toughness of PLA. The elongation at break (52.4%) of PLA/10%GOH increased by six times and the notched impact strength (5.6 kJ/m^2) increased by 86.7% **(Figure 3h**) [57].

iii. Compound modification

Compound modification is a simple method for physically blending APP with other fillers to achieve flame retardancy in PLA. Recently, Yin et al. mixed CNF as a surface modifier with APP via ball milling to prepare a hybrid FR (APP@CNF). PLA/5%APP@CNF achieved a LOI of 27.5% and also passed the UL-94 V-0 rating. The presence of CNF improved the dispersion of APP in the matrix, and 5 wt% of APP@CNF increased the impact strength of the PVA matrix by 54% **(Figure 3i**) [58]. Jia et al. used an ionic liquid (IL), tetrabutylphosphonium tetrafluoroborate, as a synergist for APP to simultaneously prepare PLA composites with flame retardancy, good toughness, and transparency (**Figure 3j**). 1.5 wt% IL and 1.5 wt% APP imparted PLA an LOI of 27.2%, a UL 94 V-0 rating, and an ultrahigh elongation at a break of 204.6% (8.5% for PLA) [47]. Xu et al. directly added ESO and APP to PLA. They prepared a PLA-based FR with a high tensile strength (42.0 MPa), high extensibility (165%), and a high

LOI of 30.2% via in-situ manipulation of interphase reactions among ESO, APP, and PLA **(Figure 3k)** [59].

Table 2. Typical flame retardant and mechanical property parameters of PLA/filler composites.

Year	**Fillers**	**Types and mechanisms of FRs**	**Impact strength (GPa)**	**Young's modulus (GPa)**	**Elongation at break (%)**	**Tensile Strength (MPa)**	**pHRR (kW/m^2)**	**THR (MJ/m^2)**	**UL-94**	**LOI (%)**	**TTI**	**FRI**	**Rank[#]**	**Ref**
2019	15% A-A (APP+ASC)	P-based (C/G cases)^	-	-	+26.3% (8.7)	−12.0% (46.3)	−39.4%	−27.7%	V0	30.5	26(35)	1.7	Good; P	[51]
2021	5% B-APP	B–P-based (C/G cases)	+62.2% (1.07)*****	-	+113.0% (19.6)	−16.0% (49.7)	−3.7%	−17.3%	V0	29.4	30(33)	1.1	Good; P	[52]
2019	5% BSi-APP	Si–B–P-based (C/G cases)	-	-	-	-	−17.6%	−26.9%	V0	26.7	33(39)	1.4	Good; -	[53]
2019	5% PC@APP	P–N-based (C/G cases)	+34.3% (4.7)	-	+106.2% (14.4)	−4.9% (50.4)	−20.1%	−2.0%	V0	28.3	32(35)	1.2	Good; P	[54]
2021	5% MAPP	P–N-based (C/G cases)	-	-	+2042.8% (150)	−14.6% (65.8)	−9.5%	−7.6%	V0	25.5	57(62)	1.5	Good; P	[55]
2019	10% APP@CS@PA-Na	Intumescent (C/G cases)	+17.1% (4.1)	−15.3% (0.7)	+28.4% (8.1)	−20.1% (45.3)	-33.0%	-19.4%	V0	30.5	71(71)	1.8	Good; P	[45]

2020	10% APP@CS@AA-3BL	Intumescent (C/G cases)	+22.8% (4.3)	−14.1% (0.7)	+20.9% (9.8)	−18.1% (46.4)	−23.1%	−10.4%	V0	+30.6	73(71)	1.5	Good; P	[56]
2018	10% GOH	Intumescent (C/G cases)	+86.7% (5.6)	No change	+555.0% (52.4)	−20.4% (39.3)	−27.7%	−24.7%	V0	-	64(64)	2.5	Good; P	[57]
2018	5% APP@CNF	P-based (C/G cases)	+54.4% (11.8)	+7.6% (2.7)	−26.2% (5.9)	−10.4% (50.3)	−13.6%	−19.2	V0	27.5	48(69)	1.0	Good; P	[58]
2020	3% IL+APP	P-based (C/G cases)	+118.2% (4.8)	−3.9% (1.6)	24 times	−6.4% (65.9)	−20.7%	−22.4%	V0	27.2	52(67)	1.1	Good; P	[47]
2020	7% ESO/APP	P-based (C/G cases)	+49.3% (4.3)	−8.8% (2.3)	20 times	−28.8% (42.0)	−50.3%	−28.4%	V0	30.2	65 (69)	2.6	Good; P	[59]

Note: + indicates increasing and – indicates decreasing, ^The flame retardant mechanism exerted by FRs is represented by the C case (the condensed phase flame retardant mechanism) and the G case (the gas phase flame retardant mechanism), * the values in brackets are the specific performance data of the modified PLA material, p-amino-benzenersulfonic acid (ASC), boron-containing APP (B-APP), microencapsulated APP with polyborosiloxane (BSi-APP), biopolyelectrolyte (PC); melamine polyphosphate (MAPP), alginate (AA), the number of assembled layers (BL), GOH is prepared by polyethyleneimine (PEI), bio-based polyelectrolyte (BPE), and graphene oxide (pGO), ionic liquid (IL); and epoxidized soybean oil (ESO), #The “Poor,” “Good,” or “Excellent” ranks are assessed for the cases based on the Flame Retardancy Index (FRI) results; P and N indicate the positive and negative effects of FRs on the mechanical properties of PLA composites, respectively.

3.2.2. Sheet-like nanofillers

Sheet-like nanofillers have attracted considerable attention because of their high specific surface areas, unique physicochemical properties, and good building blocks for nanoscale architectures. Hexagonal boron nitride (h-BN), transition metal dichalcogenides, and other 2D materials have been used to enhance flame retardancy, and the thermal and electrical properties of polymers [62, 63]. **Figure 4** shows the selected representative findings of sheet-like nanofillers for PLA. Their mechanical properties and flame retardancy indices are summarized in **Table 3**.

The introduction of clay, talc, carbon nanotubes (CNTs), graphene, graphene oxide (GO), polyhedral oligomeric silsesquioxane (POSS), and cellulose nanocrystals as nanofillers to enhance the performance of PLA is a simple, convenient, and adaptable method, despite their unattained biodegradable or sustainable performance [64, 65]. h-BN shows high biocompatibility, thermal conductivity (60 W/mK), chemical and thermal stability, and oxidation resistance [66, 67]. It is a promising nanofiller for the preparation of polymeric nanocomposites with integrated performances. PA, one of the most attractive P-containing biomass materials, has been used as an environmentally friendly bio-based FR for polymers to synthesize various polymeric or hyperbranched efficient FRs by relying on its six highly active phosphate groups [68, 69]. The multifunctional nanofillers of P-rich PA-functionalized h-BN (f-BNNSs) improved the flame retardancy and thermal conductivity of PLLA. The flame retardancy of PLLA was improved by adding 20 wt% of f-BNNSs, and the LOI value increased from 18.5% of PLLA to 27.5% (**Figure 4a**) [70].

Phosphazene, a two-dimensional nanosheet with high thermal stability and a unique phosphorus–nitrogen alternating molecular structure, was modified by PA to enhance interfacial compatibility and flame retardancy (**Figure 4b**). Yang et al. obtained a microporous nanosheet IFR via the self-assembly of PA and hexakis (4-aminophenoxy) cyclotriphosphazene (HACP-PA) without a templating agent, which significantly improved purification. Adding 5 wt% HACP-PA to PLA achieved a UL-94 V-0 rating and the LOI was 24.2% [71].

Montmorillonite, layered double hydroxides (LDHs), and sepiolite, types of 2D clay nanomaterials, are fire and high-temperature resistant, absorb water and swell, and have excellent ion-exchange capacity. Hence, they have been used as preferred materials in reinforcing polymers [72, 73]. They can be modified by intercalation, filling, blending, and adsorption to improve the dispersibility of substrates. LDHs, also known as hydrotalcite-like or anionic clays, are hydroxides with layered crystal structures composed of two or more metals [74, 75]. The LDH nanofiller sheet does not peel off easily because of the strong electrostatic force between the highly charged hydroxide and anionic intercalation layers. Therefore, it is difficult to be dispersed in the PLA matrix [76, 77].

Zhang et al. used a reconstruction method to prepare phosphotungstic acid-intercalated MgAl-LDH to reduce the additional IFR and effectively improve the flame retardancy of PLA **(Figure 4c)**. PLA containing 18.0 wt% IFR and 2.0 wt% modified LDH achieved a maximum LOI value of 48.3%, cleared the UL-94 V-0 rating, and significantly reduced the pHRR by 86.9% [76]. Jia et al. prepared DOPO–calcium montmorillonite (Ca-MMT) nanocomposites by intercalating DOPO into Ca-MMT (**Figure 4d**). The PLA/ DOPO-Ca-MMT nanocomposites exhibited higher crystallinity, higher LOI, and lower pHRR than those of PLA/DOPO and PLA/ Ca-MMT [78]. MXene, a new layer-structured material, has attracted attention because of its high aspect ratio and stiffness, which can affect the stalling behavior of polymer chains during processing and enhance the mechanical properties of the matrix [73, 79]. MXene and 2D transition metal carbide/nitride nanosheets can endow polymers with excellent flame retardancy by suppressing heat and mass exchange between the gas and solid phases during combustion. The simultaneous addition of 1.0 wt% MXene and 11.0 wt% IFR to PLA enhanced the LOI of PLA/IFR from 21.5% to 34.5%, decreased the pHRR (64.6%), and cleared the V-0 grade in UL-94 test [80]. MXenes, similar to other 2D materials, are limited by intermolecular van der Waals forces during the assembly process, resulting in sheet stacking and overlapping. Surface modification and heteroatom doping have addressed the loss of surface utilization due to 2D stacking [81,82]. Shi et al. used benzyldimethylhexadecyl ammonium chloride (HDBAC)-modified titanium carbide ($Ti_3C_2T_x$) ultrathin nanosheets and FR PLA together with ammonium polyphosphate (SiAPP) filled with silicon microcapsules (**Figure 4e**). 2.0 wt% HDBAC-$Ti_3C_2T_x$ (HD-TC) and 13.0 wt% SiAPP increased the LOI value of PLA to 33.3%, achieving a UL-94 V-0 rating. The barrier and catalytic effects of the modified $Ti_3C_2T_x$ nanosheets significantly inhibited the formation of the toxic gases. The TSP of the composite decreased by 52.7% [83]. Xue et al. fabricated a novel MXene-phenyl phosphonic acid diaminohexane (MXene-PPDA) nanohybrid by embedding PPDA into an MXene interlayer. Adding 1.0 wt% MXene-PPDA cleared the UL-94 V-0 rating of PLA with a 22.2% reduction in the pHRR. Besides, the composite enhanced the elongation at break and impact strength of the PLA matrix by ~173.4% and 11.1%, respectively **(Figure 4f)** [84].

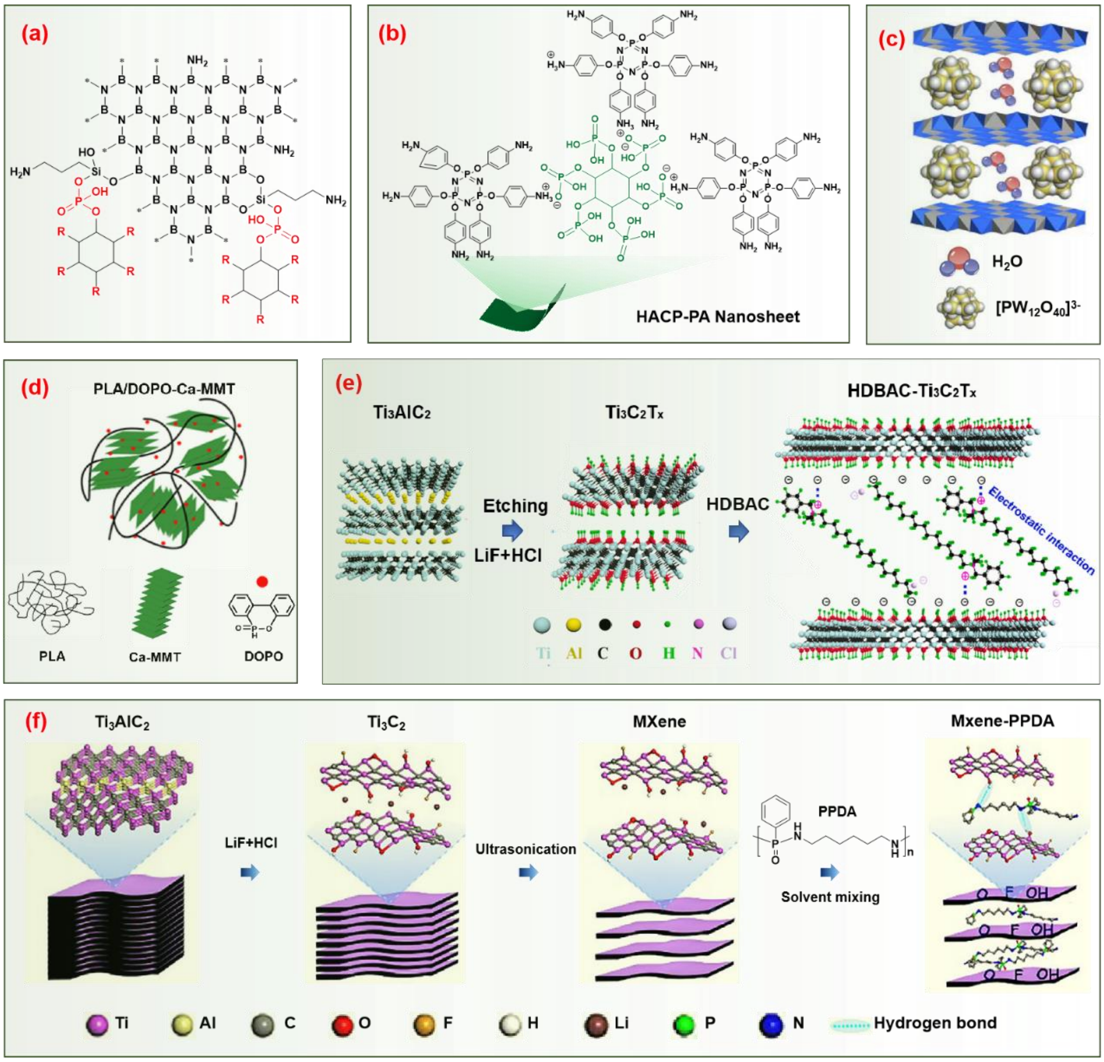

Figure 4. The typical nanosheet flame retardant: (a) Chemical structure of f-BNNSs (redrawn from reference [70]; copyright (2020) ACS). Schematic diagram for the preparation of (b) HACP-PA microporous nanosheet (redrawn from reference [71]; copyright (2021) Elsevier) and (c) PWA-LDH (redrawn from reference [76]; copyright (2018) Elsevier). (d) Illustrations of the intercalating states of PLA/DOPO-Ca-MMT (redrawn from reference [78]; copyright (2019) Wiley). Schematic diagrams for the synthesis of (e) HDBAC-$Ti_3C_2T_x$ (redrawn from reference [83]; copyright (2022) Elsevier) and (f) MXene-PPDA (redrawn from reference [84]; copyright (2020) Elsevier).

Table 3. Typical flame retardant and mechanical property parameters of PLA/nano/micro filler composites.

Year	Fillers	Types and mechanisms of FRs	Impact strength (GPa)*	Young’s modulus (GPa)	Elongation at break (%)	Tensile Strength (MPa)	pHRR (kW/m^2)	THR (MJ/m^2)	UL-94	LOI (%)	TTI	FRI	Rank#	Ref
2020	20% f-BNNSs (Figure 4a)	B–P–N-based (C/G cases)^	-	-	-	-	-	−39.9% (9.8 KJ/g)	-	27.5	-	-	-;-	[70]
2021	5% HACP-PA (Figure 4b)	P–N-based (C/G cases)	-	-	−15.4% （2.2）	−19.7% （27.2）	−15.3%	−21.5	V0	24.2	57 (68)	1.0	Good; N	[71]
2018	18.0% IFR + 2.0% PWA-LDH (Figure 4c)	Intumescent (C/G cases)	-	-	−40% (1.5)	−56.1% (24.6)	−86.9%	−65.8%	V0	48.3	26 (41)	14.6	Excellent; N	[76]
2019	DOPO/Ca-MMT (Figure 4d)	Mineral & P-based (C/G cases)	-		+35.7% （8.6）	−2.8% （66.0）	−14.9%	−3.8%	V0	28.3	33 (35)/27 (34)	1.1/0.9	Good/Poor; P	[78]
2020	11% IFR + 1% MXene	Intumescent (C/G cases)	-	-	-	-	−64.6%	−16.5%	V0	34.5	35 (37)	3.2	Good; -	[80]
2022	2.0% HD-TC + 13.0% SiAPP (Figure 4e)	P–N–Si-based (C/G cases)	-	-	-	-	-49.9%	−32.0%	V0	33.3	50 (60)	2.5	Good; -	[83]
2020	1% MXene-PPDA (Figure 4f)	P–N-based (C/G cases)	+11.1% (3.5)	-	+173.4% (29.8)	+1.2% (57.8)	−22.2%	−6.2%	V0	22.8	59 (64)	1.3	Good; P	[84]

Note: + indicates increasing and – indicates decreasing, ^The flame retardant mechanism exerted by FRs is represented by the C case (the condensed phase flame retardant mechanism) and the G case (the gas phase flame retardant mechanism), * the values in brackets are the specific performance data of the modified PLA material, PA-functionalized hexagonal boron nitride (f-BNNSs), self-assembly of PA and hexakis (4-aminophenoxy) cyclotriphosphazene (HACP-PA), phosphotungstic acid-intercalated MgAl-LDH (PWA-LDH); benzyldimethylhexadecylammonium chloride -modified MXene (HD-TC), and phenyl phosphonic acid diamino-hexane (PPDA). #The “Poor,” “Good,” or “Excellent” ranks are assessed for the cases based on the Flame Retardancy Index (FRI) results; P and N indicate the positive and negative effects of flame retardants on the mechanical properties of PLA composites, respectively.

3.2.3. Carbon-based fillers

Carbon nanomaterials have been regarded as a frontier of scientific and technological exploration owing to their low density, large specific surface areas, high mechanical strength, chemical stability, biological activity, and biocompatibility. Graphene [86, 87], CNTs [85, 86], fullerene (C_{60}) [90, 91], and nanocarbon black (NCB) [92] were used as nanoFR systems [85] to improve the char-forming ability of the matrix. They exhibited good thermal and mechanical stabilities. This section presents the representative research on carbon-based fillers in PLA. The relevant mechanical and flame retardancy performance indices are summarized in **Table 4**.

Since its discovery in 2004, graphene has rapidly become a research topic owing to its unique structure and excellent physical and chemical properties [93]. Natural graphite is oxidized by strong oxidants such as perchlorate, sulfuric acid, and nitrate to form graphite oxide (GO), a compound with a quasi-2D layered structure [48]. A large number of hydrophilic active groups (hydroxyl, epoxy, and carboxyl groups) are present between the layers and the GO surface. The hydrophilic groups impart negative charges to the GO sheets. These sheets combine with organic cations and expand the interlayer spacing of GO. The GO surface changes from hydrophilic to the lipophilic surface through organic modification, which reduces the activation energy of its surface and improves compatibility and adhesion with other polymers [94,95]. Functionalizing GO with long-chain polyester and interfacial modification with binary matrix 2D-LDH prevents severe agglomeration, promotes charring, and reduces CO_2 emission during combustion, endowing PLA with excellent mechanical properties and flame retardancy **(Figure 5a)** [77]. GO in polymers cannot achieve the expected flame retardancy alone; therefore, it is often combined with other high-efficiency FRs. **Figure 5b** shows the novel additive PMrG obtained by the self-assembly of melamine and PA onto reduced graphene oxide (RGO). The additive effectively inhibited the release of heat and smoke from PLA due to the decomposition of PA and melamine to produce nonflammable volatiles and the synergistic effect of the three components [96]. Another composite was obtained by aryl-grafting azoboron (AZOB) onto GO, followed by in-situ reduction/intercalation with sodium metaborate (SMB) (**Figure 5c**). Modified RGO improved the flame retardancy, smoke suppression, and mechanical properties of PLA nanomaterials. The peak heat release rate and total smoke release of the final material decreased by 76.5% and 55.6%, respectively with a 49.1% increase in the tensile strength [98]. Yu et al. proposed a strategy to improve the dispersion of GO and enhance its flame retardancy. The coordinated unsaturated metal sites in the metal–organic framework (MOF) were atomically dispersed and used as highly active sites in different reactions: catalysis, separation, and sensing. It is commonly modified with MOFs as shown in **Figure 5d**. Details are provided in *section 3.2.4*. A core–shell GO hybrid (BCSGOH) was prepared by encapsulating a FR (APP as the core, CS, and PA salt (PA-Na) as the outer shell) with polyethyleneimine-modified GO as the shell. 6 wt% BCSGOH provided PLA with UL94 V-0 rating, a high LOI value of 30.0%, and a notched impact strength of 12.38 kJ/m^2 **(Figure 5e)** [86]. Branched functionalized graphene (PNFR@RGO) was fabricated by chemically functionalizing RGO with branched polyethylenimine (BPEI) and DOPO (**Figure 5f**)[97]. After adding 4 wt% PNFR@RGO, the degradation temperature of PLA in the air increased, the heat release rate (HRR) decreased, and the total smoke emission (TSR) was significantly inhibited by 79%.

Apart from GO, the modification of carbon-based filters with FR PLA has emerged in recent years (**Figure 5g-i**) [99,100]. Grafting FRs containing P and N onto the surface of carbon-based nanomaterials had significant flame-retardant efficiency and improved mechanical properties [101]. Yang et al. synthesized calcium magnesium phytate (CaMg-Ph) by reacting calcium chloride and magnesium chloride with biological PA. Compared to 20 wt% CaMg-Ph, the addition of 19 wt% CaMg-Ph and 1 wt% CNT to PLA resulted in a slight increase in the tensile strength (52.8 MPa), a better flame retardancy with a lower pHRR (35.0%), and a higher carbon residue (18.4 wt%) [102]. A nanofiller hybrid (CB-g-DOPO) obtained by the functional modification of nanoscale carbon black (CB) via H_2O_2 hydroxylation and chemical grafting of DOPO improved the comprehensive performance of the PLA nanocomposite. The PLA was imparted with excellent electrical conductivity by 4 wt% CB-g-DOPO **(Figure 5h)** [103]. Cao et al. synthesized graphitic carbon nitride (g-$C_3N_{4)}$ via the thermal decomposition of melamine and introduced it to PLA in combination with DOPO. The synergetic effects of g-C_3N_4 with DOPO resulted in a dense char layer with a high degree of graphitization, improved thermal stability, and flame retardancy of PLA [104].

Table 4. Typical flame retardant and mechanical property parameters of PLA/filler composites.

Year	Fillers	Types and mechanisms of FRs	Impact strength (GPa)	Young’s modulus (GPa)	Elongation at break (%)	Tensile Strength (MPa)	pHRR (kW/m^2)	THR (MJ/m^2)	UL-94	LOI (%)	TTI	FRI	Rank[#]	Ref
2021	5 wt% d2D-Gc (Figure 5a)	Metal-containing & C-based (C cases)	-	+14.2% (1.8) *	−48.3% (176.3)	+2.2% (25.6)	−40.9%	−5.4%	-	-	-	-	-; N	[77]
2021	10% PMrG (Figure 5b)	P–N-based & C-based (C/G cases)	-	-	-	-	−35.3%	−20.9%	V0	25.0	59 (74)	1.5	Good; -	[96]
2019	2% PNFR@RGO (Figure 5f)	P–N-based & C-based (C/G cases)	-	-	-	-	−25.0%	−19.0%	-	-	-	-	-; -	[97]
2019	2% RGO-AZOB/SMB (Figure 5c)	B–N-based & C-based (C/G cases)	-	+34.9%	−60.8%	+49.1	−76.5%	−76.9%	V0	31.4	43 (29)	27.3	Excellent; P	[98]
2022	8% BCSGOH (Figure 5e)	Intumescent & C-based (C/G cases)	+22.8% (9.6)	+0.5% (3.9)	−33.2% (4.6)	−26.7% (43.6)	−35.6%	−6.2%	V0	30.8	47 (62)	1.2	Good; N	[86]
2018	4% DVCNT	P–Si-based & C-based (C/G cases)	-	-	-	-	−29.8%	-	V1	26.6	-	-	-; -	[99]
2018	1% MWCNT–DOPO-OH+24% AHP	P-based & metal-containing & C-based (C/G cases)	-	-	-	-	-	-	V0	32.3	-	-	-; -	[100]
2021	20% BC-m	P–N-based & C-based (C/G cases)	-	+21.5% (0.9)	-	−10.6% (51.9)	−53.8%	−37.8%	V0	29.2	31 (56)	2.8	Good;P	[101]
2018	19 wt% CaMg- Ph+1 wt% CNT (Figure 5g)	P-based & metal-containing & C-based (C/G cases)	-	-	−36.4% (2.1)	−4.8% (52.8)	−35.3%	−11.7%	-	-	51 (66)	1.3	Good; N	[102]
2020	8% CB-g-DOPO (Figure 5h)	P-based & C-based (C/G cases)	+146% (10.1)	+27.2% (2.0)	7.6 times (44.2)	+18.2% (66.8)	−40.3%	−18.5%	V0	28.6	31 (47)	1.3	Good; P	[103]

2020	5% g-C$_3$N$_4$+5%DOPO (Figure 5i)	P-based & C-based (C/G cases)	-	−1.6% (1.3)	−51.3% (3.6)	−33.2% (38.8)	−15.3%	−8.7%	V0	26.5	83 (65)	1.6	Good; N	[104]
2018	0.5 wt% nano-ZIF-8@GO	Metal-containing & C-based (C/G cases)	-	-	+38.5% (24.1)	+36.4% (49.63)	-	-	V2	24.0	-	-	-; P	[105]

Note: + indicates increasing and – indicates decreasing, ^The flame retardant mechanism exerted by FRs is represented by the C case (the condensed phase flame retardant mechanism) and the G case (the gas phase flame retardant mechanism), *the values in brackets are the specific performance data of the modified PLA material, dual-2D LDH-anchored polyester-functionalized graphene (d2D-Gc), self-assembly of melamine and PA onto reduced graphene oxide (PMrG), RGO functionalized with branched polyethylenimine and DOPO (PNFR@RGO), aryl-grafting of azoboron on GO followed by in-situ reduction/intercalation with sodium metaborate (RGO-AZOB/SMB), encapsulating CSFR (APP as the core, chitosan and phytic acid salt as the outer shell) with polyethyleneimine-modified GO (BCSGOH), multiwalled carbon nanotubes modified using DOPO and vinyl triethoxy silane (DVCNT), DOPO grafted onto the surfaces of multiwalled carbon nanotubes (MWCNT–DOPO-OH), aluminum hypophosphite (AHP), phosphate- and urea-grafted bamboo charcoal (BC-m), calcium chloride and magnesium chloride reacted with PA (CaMg-Ph), carbon black chemical grafted by DOPO (CB-g-DOPO), graphitic carbon nitride (g-C$_3$N$_4$), and nano-ZIF nanoparticles anchored on GO sheet (nano-ZIF-8@GO), #The "Poor," "Good," or "Excellent" ranks are assessed for the cases based on the Flame Retardancy Index (FRI) results; P and N indicate the positive and negative effects of flame retardants on the mechanical properties of PLA composites, respectively.

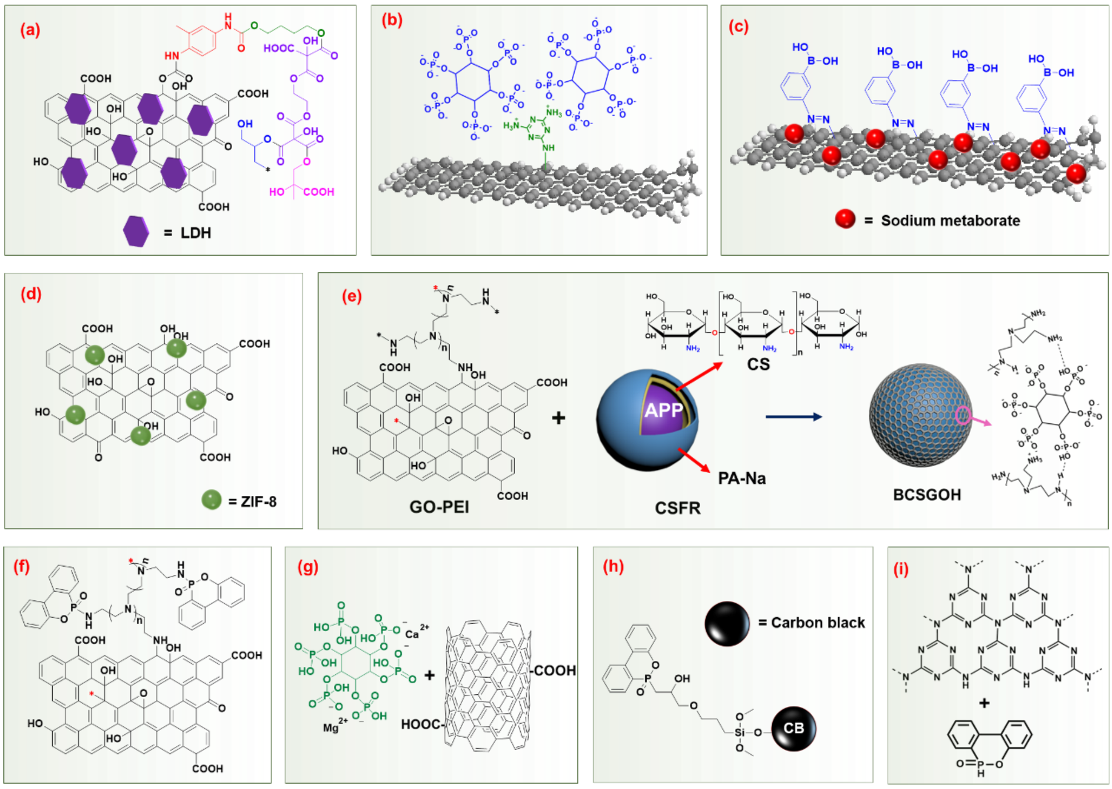

Figure 5. Schematic illustration of fabrication of (a) dual-2D LDH-anchored PG (redrawn from reference [77]; copyright (2021) Elsevier), (b) PMrG (redrawn from reference [96]; copyright (2021) MDPI), (c) RGO-AZOB/SMB hybrid (redrawn from reference [98]; copyright (2019) Elsevier), (d) ZIF-8@GO (redrawn from reference [105]; copyright (2018) Springer Link), (e) core–shell GO hybrid (BCSGOH) fabrication (redrawn from reference [86]; copyright (2022) Elsevier), (f) PNFR@RGO (redrawn from reference [97]; copyright (2019) Elsevier), (g) CaMg-Ph and acid treated MWCNT (redrawn from reference [102]; copyright (2018) Elsevier), (h) CB-g-DOPO (redrawn from reference [103]; copyright (2020) Elsevier), and (i) $g\text{-}C_3N_4$ with DOPO (redrawn from reference [104]; copyright (2020) Wiley).

3.2.4. Metal-containing fillers

Metal-containing fillers, a class of common inorganic nanoparticles, are nontoxic, stable, and reduce the amount of smoke generated during plastic combustion. Thus, they have great potential as FR PLA. Wang et al. introduced melamine zinc phytate (MPAZn) in PLA and found that the pHRR of PLA composites decreased by 45.0% with a loading of 20 wt%; the addition of Zn reduced the TSR by 81.3% than PLA/ melamine phytate (MPA) 20 [106]. The compatibility between polymers and metal oxides is poor. Most metal oxides need to improve their flame retardancy at the expense of their mechanical properties. There are a few restrictions on the blendability of organic FRs and polymers. Thus, metal–organic FRs combine the advantages of organic and metal-containing FRs to compensate for this deficiency. **Table 5** summarizes the results for metal-containing FRs used in PLA. The typical structures and compositions of the additives are shown in **Figure 6**.

APP, a highly efficient phosphorus-containing inorganic compound, exhibits excellent synergistic performance as an FR with metal oxides. Nano-zinc oxide (nano-ZnO) is an effective synergist for IFR. Xu et al. introduced nanoZnO into a phosphazene/triazine double-based FR via in-situ doping. The composite improved the carbon-forming ability and flame retardancy of PLA while maintaining its mechanical properties **(Figure 6a)** [107]. A novel nanorod-like composite FR (NRH-FR) was synthesized by reacting phenyl phosphinic acid (BPA) with powdered aluminum hydroxide (**Figure 6b**). This prevented the carboxyl groups in BPA from depolymerizing PLA molecules during melt processing, thereby improving the compatibility of additives with the matrix. The prepared nanocomposites exhibited better mechanical and FR properties than PLA [108]. **Figure 6c** shows the synthesis of a bio-based

FR (ATMP-NA-Fe) using amino trimethylene phosphonic acid (ATMP), nicotinamide (NA), and $FeCl_3$•$6H_2O$ as raw materials via a simple water–ion reaction. A total loading of 10 wt% ATMP-NA-Fe and APP in the ratio of 1:1 increased the LOI of PLA to 32.8%, whereas the pHRR and average weight loss rate decreased by 66.4% and 76.7%, respectively. Young's modulus of the final PLA increased by 46.8% [109]. Sundar prepared a zirconium dioxide (ZrO_2)-modified PLA biocomposite film. Surface treatment through Schiff bonds (SB) enhanced the dispersibility of ZrO_2 particles in the PLA matrix imparting high Young's modulus to PLA and significantly increasing the tensile strength with a 3 wt% concentration, resulting in a UL-94 V-0 rating for the PLA film **(Figure 6d)** [110].

Nanomaterials with self-charring and self-catalyzing functions are high-performance synergists for different FR polymeric matrices. MOFs are emerging porous materials composed of metal ions linked by organic bridging ligands. The organic segments of nano-MOFs interact strongly with polymer chains making the MOF compatible with polymers. The metal in MOFs catalyzes combustion, promotes the char formation of the polymer, and simultaneously releases inflammable gases to inhibit combustion. MOFs capture volatile organic compounds (VOCs) produced via polymer decomposition, thereby reducing the release of harmful substances during combustion. Wang synthesized Ni-MOF nanosheets as potential carbonization agents. Schiff bases and polyhydroxy structures were included in the organic framework to improve the charge-forming ability of Ni-MOF. The synthesized Ni-MOF and APP were used as IFR formulations to improve the flame retardancy of PLA **(Figure 6e)** [111]. Zhang et al. obtained mesoporous nickel phosphate (Ni-PO) by introducing Na_3PO_4 into MOFs using a facile template hydrothermal method. The substitution of 5 wt% APP by Ni-PO in PLA suppressed the TSP during combustion (reduced by 43%). Both the tensile and impact strengths of final composites were improved **(Figure 6f)** [112]. Apart from the Ni-containing MOF, the nano-ZIF-8 [Zn(MeIm)$_2$, MeIm = 2-methylimidazole], a zeolitic imidazole framework containing up to 24.6 wt% nitrogen and a large amount of zinc, showed good synergistic FR effect. **Figure 6g** shows that the PLA film prepared with the nano-ZIF-8@GO hybrid using nano-ZIF-8 modified GO and resorcinol diphosphate (RDP) featured good tensile strength and flexibility. The LOI of the PLA nanocomposite film was more than 27.0% achieving a VTM-0 level [113]. Zhang et al. designed ternary hybrid nanoflakes (GPZ) using a simple two-step strategy based on GO, phenylphosphinic acid (PPA), and nanoscale MOF (nano-ZIF-8) particles. The addition of 2.0 wt% GPZ significantly reduced the pHRR of PLA by 39.5% compared to that of pure PLA. The sample showed a noticeable reinforcement effect, and its tensile strength and toughness were 44.1 MPa and 86.0 MPa, respectively **(Figure 6h)** [114].

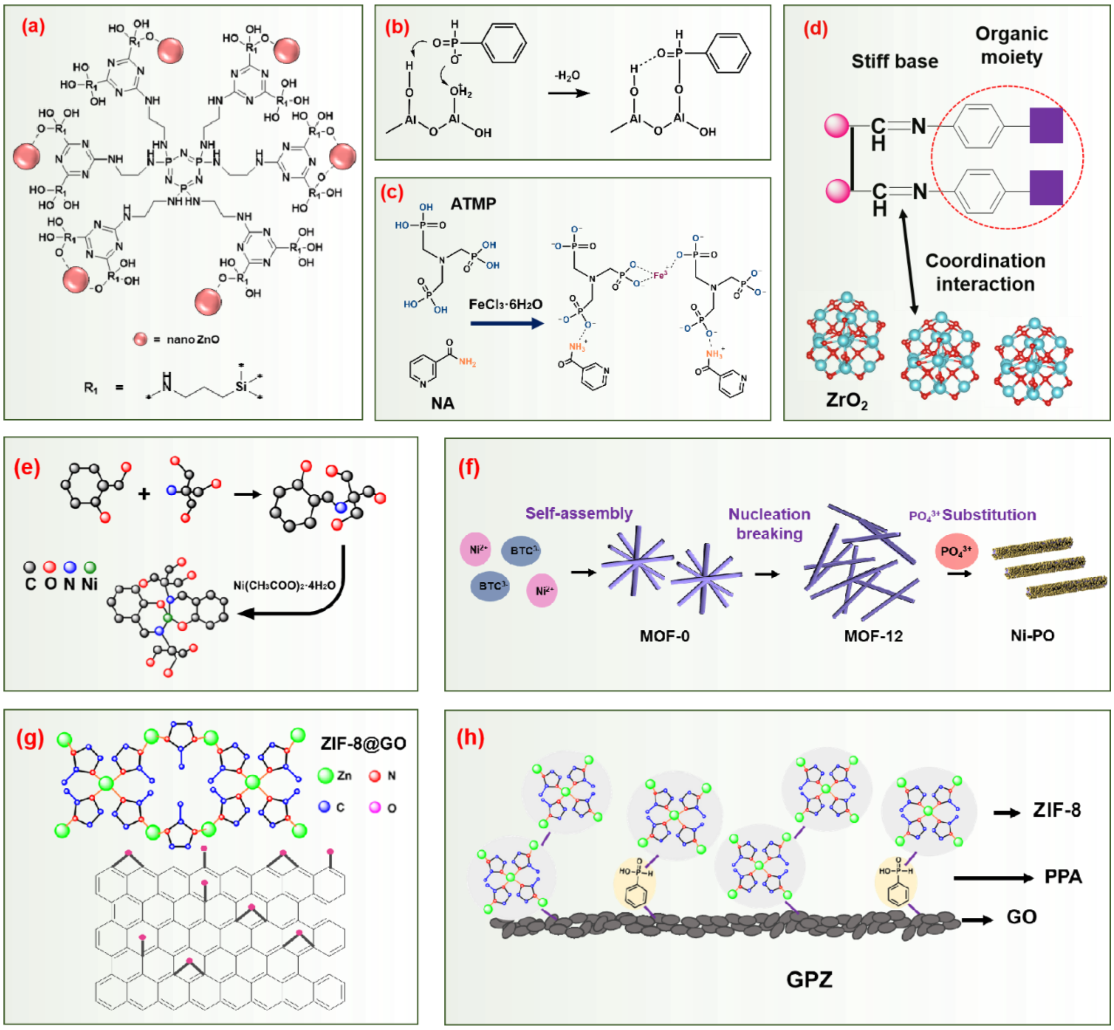

Figure 6. Schematic illustration of chemical structures of (a) A4-d-ZnO (redrawn from reference [107]; copyright (2019) Wiley), (b) NRH-FR (redrawn from reference [108]; copyright (2016) RSC), (c) ATMP-NA-Fe (redrawn from reference [109]; copyright (2021) Elsevier), (d) Stiff Base treated ZrO_2 (redrawn from reference [110]; copyright (2021) Elsevier), (e) Ni-MOF (redrawn from reference [111]; copyright (2020) Elsevier), (f) Ni-PO (redrawn from reference [112]; copyright (2019) Wiley), (g) ZIF-8@GO (redrawn from reference [113]; copyright (2018) MDPI), and (h) GPZ (redrawn from reference [114]; copyright (2020) Elsevier).

Table 5. Typical flame retardant and mechanical property parameters of PLA/filler composites.

Year	**Fillers**	**Types and mechanisms of FRs**	**Impact strength (GPa)**	**Young's modulus (GPa)**	**Elongation at break (%)**	**Tensile Strength (MPa)**	**pHRR (kW/m^2)**	**THR (MJ/m^2)**	**UL-94**	**LOI (%)**	**TTI**	**FRI**	**Rank[#]**	**Ref**
2019	5% A4-d-ZnO (Figure 6a)	P–N-based & metal-containing (C/G cases)	−11.5% (10.8) *****	-	−3.8% (2.5)	−28.0% (36.2)	−31.2%	−3.7%	V2	24.0	-	-	-; N	[107]
2016	20% NRH-FR (Figure 6b)	P-based & metal-containing (C/G cases)	-	-	-	-	-	-	V0	23.0	-	-	-; -	[108]
2021	10 wt% ATMP-NA-Fe + APP (1:1) (Figure 6c)	P–N-based & metal-containing (C/G cases)	-	+46.8% (0.91)	−42.0% (4.7)	−19.4% (44.4)	−66.4%	−14.9%	V0	32.8	29 (37)	2.7	Good; N	[109]
2021	3% SB-treated ZrO_2	N-based & metal-containing (C/G cases)	-	-	−30.0% (2.8)	+65.6% (5.3)	-	-	V0	-	-	-	-; P	[110]
2019	1.7% Ni-MOF+3.3%APP(Figure 6d)	P-based & metal-containing (C/G cases)	-	-	-	-	−26.9%	−23.9%	V0	31.0	97 (67)	2.4	Good; -	[111]
2019	5% Ni-PO+5% APP (Figure 6f)	P-based & metal-containing (C/G cases)	−25.3% (12.4)	+14.2%	-	−2.5%	−25.5%	−22.0%	V2	26.3	-	-	-; N	[112]
2018	1.2% ZIF-8@GO+9% RDP (Figure 6g)	P-based & metal-containing & C-based (C/G cases)	-	-	+64.6% (16.33)	+22.8% (47.4)	-	-	V0	27.8	-	-	-; P	[113]
2020	2% GPZ (Figure 6h)	P-based & metal-containing & C-based (C/G cases)	-	-	-	+47.0% (44.1)	−40.8%	−33.5%	V2	27.0	62 (67)	2.4	Good; P	[114]

Note: + indicates increasing and – indicates decreasing, ^The flame retardant mechanism exerted by FRs is represented by the C case (the condensed phase flame retardant mechanism) and the G case (the gas phase flame retardant mechanism), * the values in brackets are the specific performance data of the modified PLA material, nano-zinc oxide introduced into phosphazene/triazine double-base flame retardant (A4-d-ZnO), phenyl phosphinic acid reacted with powdered aluminum hydroxide (NRH-FR), the product via ion reaction among amino trimethylene phosphonic acid, nicotinamide and $FeCl_3$•$6H_2O$ (ATMP), Schiff bonds (SB), α-Phenyl-N-(2-propyl-2-hydroxymethyl-1,3-dihydroxy)-imine-Nickel (Ni-MOF), mesoporous nickel phosphate (Ni-PO), nano-ZIF-8 modified GO (ZIF-8@GO), and ternary hybrid nanoflakes prepared by GO, phenylphosphinic acid and nano-ZIF-8 (GPZ), #The "Poor," "Good," or "Excellent" ranks are assessed for the cases based on the Flame Retardancy Index (FRI) results; P and N indicate the positive and negative effects of flame retardants on the mechanical properties of PLA composites, respectively.

3.3 Small-molecule FRs

The miniaturization of various plastic devices have increased the negative effects of loading high amounts of FR additives. The weak compatibility between the FR and PLA severely degrades the mechanical properties of PLA composites [14, 115]. Small-molecule FRs enable PLA to achieve good comprehensive performance and can be integrated to develop efficient FRs. P–N FRs have been developed as ecofriendly halogen-free FR alternatives with high flame-retardant efficiency and good interfacial compatibility with polymer matrices. The FR mechanism of P–N synergy is the combined effect of the condensed and gas phases [116, 117]. The FR decomposes into inorganic acids (phosphoric and polyphosphoric acids) during combustion, which can form a protective film on the substrate surface to isolate air. Ammonia, nitrogen, water vapor, and nitrogen oxides are released. These blocks the supply of oxygen and retards combustion. Some selected representative findings for small-molecule FRs are presented in **Figure 7**. Their mechanical properties and flame retardancy performance indices are summarized in **Table 6**.

Wang et al. synthesized N, N′-bis [1-(salicylidene)methanephosphonous acid]-1,2- ethylene diamine (SHPE) by a reaction between hypophosphorous acid and a Schiff base with a high P/N content. Owing to the good flame retardancy of SHPE both in gas and condensed phases, addition of 10 wt% SHPE increased the LOI value of PLA up to 28.3%. It also increased the elongation at the break of the sample from 4.4% to 4.6%, showing a certain toughening effect **(Figure 7a)** [118]. Tawiah et al. designed a new cyclohosphorus-nitrogen FR, (hexaphenyl (nitrilotris(ethane-2,1-diyl)) tris (phosphoramidate) (HNETP) with high P and N contents. They demonstrated that only a 3 wt% loading of HNETP facilitated the V-0 rating in the UL-94 test of PLA with a significant increase in the LOI. Good dispersion and the interfacial bonding of the HNETP in the PLA matrix improved the tensile strength and Young's modulus of the sample by 67.4% and 87.8%, respectively **(Figure 7b)** [119]. Liu et al. synthesized a phosphoramide compound (PPDO) with excellent thermal stability through the nucleophilic substitution of diphenylphosphinyl chloride and piperazine to address the weak crystallization ability of PLA and simultaneously improve the fire safety and crystallinity of PLA. The incorporation of 3 wt% PPDO allowed PLA to Attain a UL-94 V-0 rating with an LOI of 27.8%. The compound is an excellent nucleating agent and increases the crystallinity of PLA, endowing it with relatively high mechanical properties and transparency **(Figure 7c)** [120]. Diphenylphosphinyl chloride was used in combination with N, N-bis(2-aminoethyl) ethylenediamine to prepare a multifunctional additive N, N’,N’’-(nitrilotris(ethane-2,1-diyl))tris(P,P-diphenylphosphinic amide) (NTPA) via substitution reaction. On account of the gas phase inhibition of benzene and phosphorus oxide radicals generated by the pyrolysis of NTPA and the certain blocking result in the condensed phase, the PLA/2.5 wt% NTPA composite reached UL-94 V-0 rating with a desirable LOI value of 28.5%. NTPA also effectively accelerated the crystallization of PLA with high crystallinity, which positively improved the strength and modulus of PLA **(Figure 7d)** [121]. Phenylphosphonic dichloride (PPDC), a common reactant in the organic synthesis of phosphorus-containing FRs, was used as a heat stabilizer for polyesters. PPDC reacted with octanol in the presence of pyridine to form octyl phenylphosphonate, a low-volatility plasticizing agent. Zhao et al. modified vanillin with PPDC to obtain a new P-containing additive, bis (5-formyl-2-methoxyphenyl phenyl phosphonate) (VP). This additive was introduced into PLA (**Figure 7e)** [122]. Tawiah et al. reacted PPDC with 2-

aminobenzothiazole to prepare a PBO-like small additive FR-phenyl-phosphonic bis (2-aminobenzothiazole) (P-ABZT) containing P, N, and S. The condensed phase mechanism of P and S components in P-ABZT and the formation of nitrogen oxides significantly reduced the heat generation during PLA combustion, increasing its LOI to 32.4% **(Figure 7f)** [123].

The preparation of small-molecule FRs from renewable resources has received considerable attention with the increasing focus on bio-based material additives. Furan is a bio-based oxygen-containing five-membered heterocyclic compound, and its derivatives promote the formation of a carbon layer in PLA during combustion. Sun et al. used furfuryl amine (FA) and phosphorus oxychloride (POC) to synthesize a multifunctional additive, furan-phosphoramide (POCFA). The LOI value of PLA increased from 19.4% to 29.6% with a V-0 rating of UL-94 for 2 wt% loading of POCFA. The presence of POCFA effectively improved the crystallinity and crystallization speed of PLA **(Figure 7g)** [124]. Ye synthesized phytic acid (PA) and furfurylamine derivative (PF), a more environmentally friendly bio-based FR, by reacting PA with FA in water. PF promoted the generation of melt droplets to remove heat while inhibiting the release of combustible products. The LOI value of the PLA composite containing 4 wt% PF was 28.5% and its pHRR was reduced by 8% **(Figure 7h)** [125]. As a reactive phosphonate intermediate, DOPO contains P–H bonds that are active with olefins, epoxy, and carbonyl groups to generate various derivatives. The application of DOPO and its derivatives as additive FRs to polymers can enhance FR efficiency and facilitate processing procedures. Long et al. synthesized three bis P–C bridged DOPO derivatives: ethyl-(DiDOPO$_1$), phenethyl-(DiDOPO$_2$), and naphthalene-(DiDOPO$_3$). These derivatives were introduced into PLA **(Figure 7i)**. 10 wt% DOPO derivatives imparted a good FR effect to the PLA composite with an acceptable V-0 rating (UL-94). The pHRR was significantly reduced. However, the rigidity of the bridging DOPO derivatives increased the flexural modulus of PLA, whereas both the elongation at break and notched impact strength was decreased [126]. Niu et al. prepared the hexa-(DOPO-hydroxymethylphenoxy-dihydroxybiphenyl)-cyclotriphosphazene (HABP-DOPO) via a substitution reaction with cyclotriphosphazene, dihydroxybiphenyl, and DOPO, and then applied it to PLA. HABP-DOPO had a rigid aromatic structure and stable P–O–C bonds, which endowed PLA with a high char-forming ability and flame retardancy. When blended with 25 wt% HABP-DOPO, PLA had an LOI of 28.5% and passed with an acceptable UL-94 V-0 rating. Meanwhile, the THR obtained from the CONE Calorimeter test also reduced dramatically by 41.7% **(Figure 7j)** [127].

POSS, a class of organic–inorganic nanoparticles, are represented as $(RSiO_{3}/_{2})_{n.}$ POSS can form a dense silicon oxide film at high temperatures owing to the stable Si–O–Si structure, which effectively prevents the escape of small molecules and droplets during the pyrogenation of polymers. It also blocks the transfer of oxygen and heat to the interior of the matrix, thus improving the FR properties of polymers [128]. Jia et al. studied the properties of PLA composites loaded with thermally stable polyhedral octaphenyl silsesquioxane (OPS) (**Figure 7k**). Although the LOI of the PLA/OPS composite was slightly lower than that of pure PLA, the pHRR and THR obtained by cone calorimetry were lower, indicating a potential FR polymer. The elongation at the break of the composite increased significantly owing to the insufficient stretching of OPS in the heat treatment process [129].

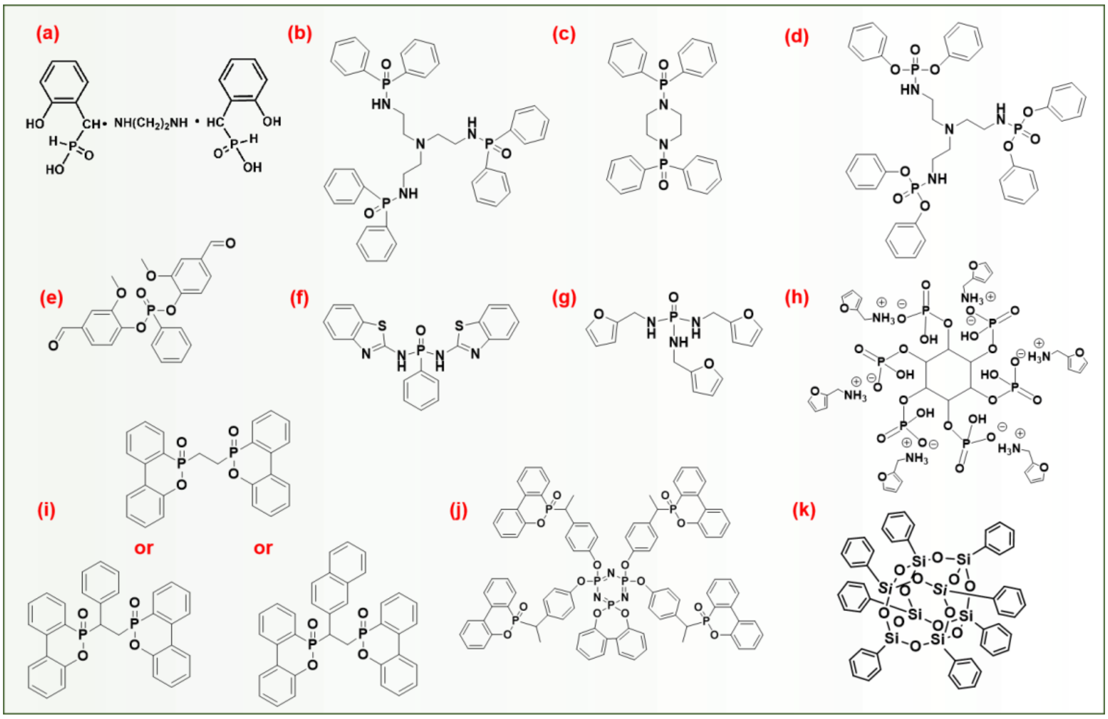

Figure 7. Chemical structure of typical small-molecule flame retardants. (a) N, N′-bis [1-(salicylidene) methanephosphonous acid]-1,2-ethylenediamine [118], (b) Cyclohosphorus-nitrogen FR-(hexaphenyl (nitrilotris(ethane-2,1-diyl)) tris (phosphoramidate) [119], (c) phosphoramide compound (PPDO) [120], (d) N, N', N''-(nitrilotris(ethane-2,1-diyl))tris(P,P-diphenylphosphinic amide) [121], (e) bis (5-formyl-2-methoxyphenyl phenyl phosphonate) [122] (f) FR-phenyl-phosphonic bis(2-aminobenzothiazole) [123], (g) POCFA (multifunctional additive furan-phosphoramide) [124], (h) bio-based flame retardant PF by reacting PA with FA[125], (i) DiDOPOx (bis P-C bridged DOPO derivatives) [126], (j) hexa-(DOPO-hydroxymethylphenoxy-dihydroxybiphenyl)-cyclotriphosphazene [127], and (k) polyhedral octaphenyl silsesquioxane [129].

Table 6. Typical flame retardant and mechanical property parameters of PLA/FR composites.

Year	Fillers	Types and mechanisms of FRs	Impact strength (GPa)	Young's modulus (GPa)	Elongation at break (%)	Tensile Strength (MPa)	pHRR (kW/m^2)	THR (MJ/m^2)	UL-94	LOI (%)	TTI	FRI	Rank[#]	Ref
2019	10 wt% SHPE (Figure 7a)	P–N-based(C/G cases)	−47.9% (5.1) *****	-	+4.5% (4.6)	−21.7% (45.4)	−30.2%	−15.3%	V0	28.3	54 (74)	1.2	Good; N	[118]
2019	3 wt% HNETP (Figure 7b)	P–N-based(C/G cases)	-	+87.8%	-	+ 67.4%	−51.3%	−43.1%	V0	32.5	57 (41)	5.0	Good; P	[119]
2020	3 wt% PPDO (Figure 7c)	P–N-based(C/G cases)	-0.5% (3.8)	-	-	−1.9% (60.8)	−14.5%	−20.1%	V0	27.8	82 (60)	1.9	Good; N	[120]
2021	2.5 wt% NTPA (Figure 7d)	P–N-based(C/G cases)	-0.6% (3.2)	-	-	−3.4% (58.3)	−2.7%	−12.2%	V0	28.5	71 (60)	1.4	Good; N	[121]
2018	5 wt% VP (Figure 7e)	P-based (C/G cases)	+12.5% (18.0)	−5.4% (3.5)	2.7times (11.0)	−5.3% (54.0)	−9.1%	−4.8%	V0	25.8	79 (68)	1.7	Good; P	[122]
2019	3% P-ABZT (Figure 7f)	P–N-based(C/G cases)	-	-	−23.0%	−30.0%	−50.0%	−37.0%	V0	32.4	85 (39)	6.2	Good; N	[123]
2019	2 wt% POCFA (Figure 7g)	P–N-based(C/G cases)	No change	+1.2% (2.6)	+1.6% (6.2)	+8.5% (89.0)	−6.8%	−2.2%	V0	29.6	80 (69)	1.3	Good; P	[124]
2021	2 wt% PF (Figure 7h)	P–N-based(C/G cases)	-	-	−19.0% (5.1)	+11.3% (47.9)	−1.9%	−2.0%	V0	28.5	51 (60)	0.9	Poor; N	[125]
2017	10% DiDOPO$_2$ (Figure 7i)	P-based (C/G cases)	-21.6% (2.9)	-	−6.1% (10.7)	−2.6% (70.4)	−13.0%	−18.0%	V0	27.1	-	-	-; N	[126]
2020	25 wt% HABP-DOPO (Figure 7j)	P–N-based(C/G cases)	-	-	-	-	−19.3%	−40.3%	V0	28.5	32 (53)	1.2	Good; -	[127]
2018	10% (heat-treated) OPS (Figure 7k)	Si-based (C/G cases)	-	-	+31.4% (8.5)	−29.1% (50.3)	−14.8%	−2.5%	-	19.4	34 (36)	1.2	Good; P	[129]

Note: + indicates increasing and – indicates decreasing, ^The flame retardant mechanism exerted by FRs is represented by the C case (the condensed phase flame retardant mechanism) and the G case (the gas phase flame retardant mechanism), * the values in brackets are the specific performance data of the modified PLA material, N, N′-bis [1-(salicylidene) methanephosphonous acid]-1,2-ethylenediamine (SHPE), Cyclohosphorus-nitrogen FR - (hexaphenyl (nitrilotris(ethane-2,1-diyl)) tris (phosphoramidate) (HNETP), phosphoramide compound, NTPA is N,N′,N″-(nitrilotris(ethane-2,1-diyl))tris(P,P-diphenylphosphinic amide) (PPDO), bis (5-formyl-2-methoxyphenyl phenyl phosphonate) (VP), FR-phenyl-phosphonic bis (2-aminobenzothiazole) (P-ABZT), multifunctional additive furan-phosphoramide (POCFA), bio-based flame retardant by reacting PA with FA (PF), bis P-C bridged DOPO derivatives (DiDOPOx), hexa-(DOPO-hydroxymethylphenoxy-dihydroxybiphenyl)-cyclotriphosphazene (HABP-DOPO), and polyhedral octaphenyl silsesquioxane (OPS). #The "“Poor,” “Good,” or “Excellent” ranks are assessed for the cases based on the Flame Retardancy Index (FRI) results; P and N indicate the positive and negative effects of flame retardants on the mechanical properties of PLA composites, respectively.

3.4 Macromolecular flame retardant

Small-molecule P/hypophosphite-based compounds and IFRs have recently shown high efficiencies in reducing the flammability of PLA. However, they suffer from low thermal stability, ease of migration, and high loading, which restrict their practical applications and can negatively affect their mechanical properties. Oligomeric- or polymer-based P-containing FRs have received increasing attention because of their high thermal stability and low migration. P/N-containing oligomeric polyphosphoramides were fabricated using two methods to improve the fire behavior and maintain the mechanical properties of PLA: condensation between phenylphosphonic dichloride and piperazine, and ion complexation between APP and CS [130, 131]. The representative findings are shown in **Figure 8**. The mechanical and flame retardancy performance indices are summarized in **Table 7**.

Wu et al. prepared a poly (phenylphosphoryl phenylenediamine) FR (PPDA) for PLA via the condensation of phenylphosphoryl dichloride (PPDCl) and p-phenylenediamine. The pHRR and THR of the PLA composites decreased with an increase in the PPDA content. The addition of less than 3 wt% PPDA to the mechanical properties of PLA made a negligible difference **(Figure 8a)** [132]. Xue et al. fabricated P- and N-containing oligomeric polyphosphoramides (PPP) from phenylphosphonic dichloride and piperazine. Only 3 wt% PPP enabled PLA to achieve UL-94 V-0 rating and an LOI value of 32.5%. The FR PLA showed a relatively low roughness with elongation at a break of 10.3%, comparable to 13.5 MPa of PLA **(Figure 8b**) [133]. A series of PPDAs with tunable structures and compositions were designed, as shown **in Figure 8c**. The addition of 1.0 wt% PPDA-8, increased the tensile strength and toughness of

PLA by 11% and 44%, respectively. The sample achieved a UL-94V-0 rating and LOI value of 26.8% [134]. Zhou et. reported FRs, as presented in **Figure 8d**, which were synthesized using phosphorus oxychloride and 4,4′-diaminodiphenyl ether (POCODA). 2 wt% POCODA blended with 10 wt% APP enhanced the char-forming ability and flame retardancy of PLA, which endowed PLA with 29% LOI values and a 30.6% drop in the pHRR [135]. Liu used triglycidyl isocyanurate (TGIC) and diethylenetriamine (DETA) as raw materials to synthesize a hyperbranched carbon agent (CT) using water as the solvent. Their study revealed that the mixing of APP with CT increased by 43.5% of the LOI value of the PLA composite with UL-94 V-0 rating and no melt dripping at a loading of 20 wt% APP/CT/aluminum hypophosphite (AHP) **(Figure 8e**) [136].

Most existing polyphosphoramide additives tend to reduce the transparency of PLA materials, and the toxic organic solvents used in the preparation process damage the environment. To address these drawbacks, Feng et al. synthesized a polyphosphoramide (DM-H) using dimethyl methylphosphonate (DMMP) and 1,6-hexanediamine (HDA) through two-step polycondensation under solvent and catalyst-free conditions. 2 wt% of DM-H could make PLA achieve an ideal V-0 rating and a high LOI value of 29.7% **(Figure 8f**) [137]. Si was introduced into polyphosphateamides (DM-Si) via polycondensation between dimethyl methylphosphonate (DMMP) and 1, 3-Bis(3-aminopropyl) tetramethyl-disloxane. DM-Si exhibited better FR performance in PLA prepared safely under nontoxic conditions. Notably, the tensile toughness of PLA improved from 2.8 MJ/m^3 to 4.7 MJ/m^3 **(Figure 8g**) [138].

Biomass (modified starch, lignin, and ramie fiber) is explored as raw materials for the preparation of sustainable bioderived polymer-based P-containing FRs. Liu et al. synthesized a novel green polyphosphate FR (PFRS) via the A2 + B3 type reaction of bisphenolic acid-based monomer (DPM, A2) and phosphorus oxychloride ($POCl_3$, B3) **(Figure 8h)**. With 3.8 wt% PFRS and 11.2 wt% APP, the resulting PLA achieved 29.7% LOI and decreased the pHRR by 46% [139]. Zhang et al. synthesized a novel bio-based PPFR (PPD) using plant-derived diphenolic acid as the raw material **(Figure 8i)**. The addition of 6 wt% of PPD enabled PLA to achieve a desirable UL-94 V-0 rating and a high LOI value of 27.1%. Besides, the PLA/6 wt% PPD showed a 31% increase in impact toughness and a slight improvement in tensile strength compared to those of PLA [14].

CS, derived from the deacetylation of natural chitin, is a nontoxic, biodegradable, and antibacterial biochemical. CS is easily carbonized owing to its multiple hydroxyl groups during combustion accompanied by the release of an inert gas to provide carbon sources and foaming agents for the FR system. PA extracted from plant tissues can combine with the NH_2 group of protonated CS under acidic conditions to form a polyelectrolyte complex through an ion reaction. CS/PA imparted FR properties to polymers through simple assembly technologies [140, 141]. Zhou et al. added an electrostatically assembled product of CS and PA (CTS/PA) to PLA. 3 wt% of the composite increased the LOI value to 30.5% and reached a UL-94 V0 level **(Figure 8j)** [142]. Li et al. designed a fully bio-based additive (PA@CHTM) with a core–shell structure, which is synthesized by CS microspheres (CHTM) and PA. The addition of 9 wt% PA@CHTM to PLA exhibited good FR properties, excellent UV resistance, and a rapid biodegradation rate in the natural environment **(Figure 8k)** [143].

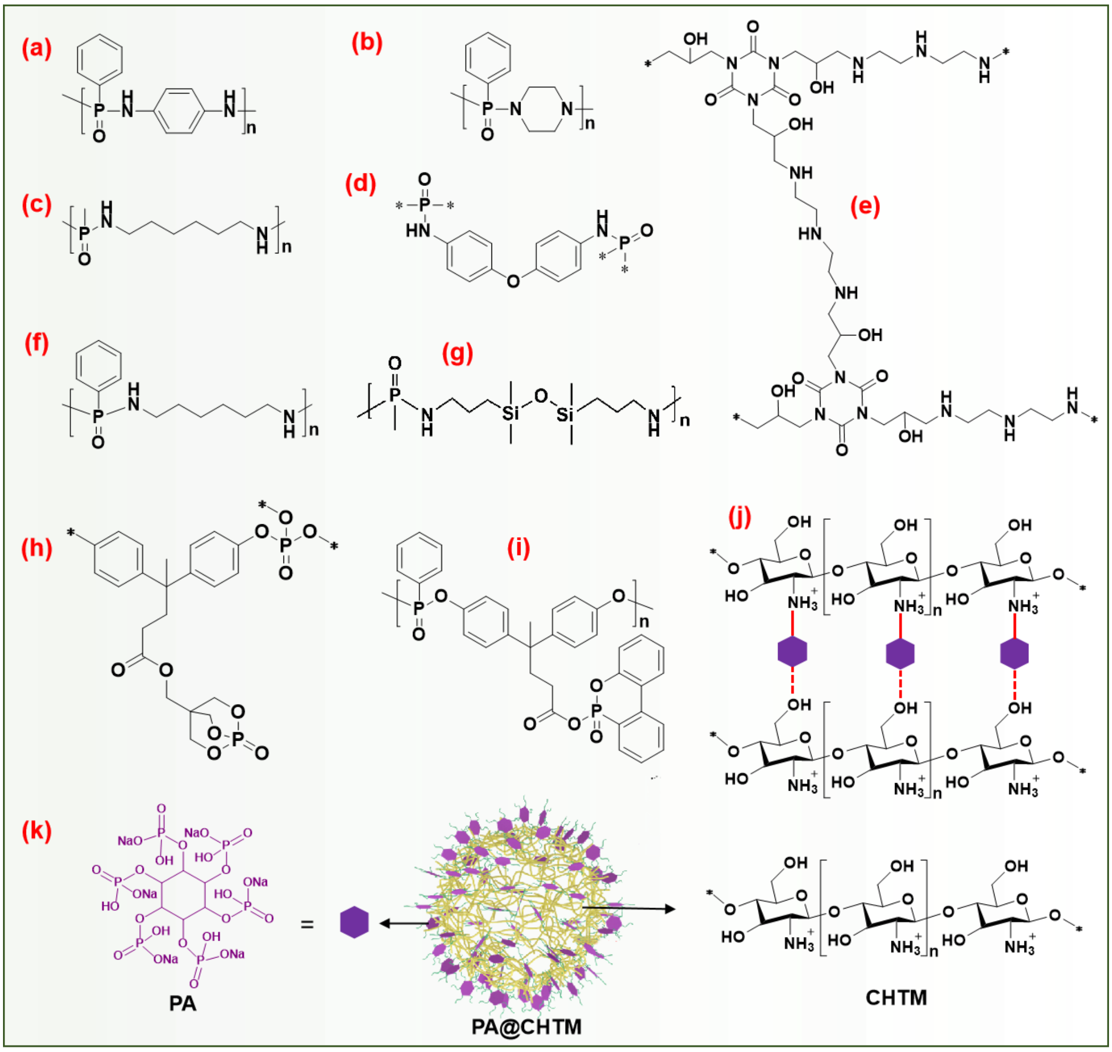

Figure 8. Chemical structure of macromolecular flame retardants: (a) poly (phenylphosphoryl phenylenediamine) [132], (b) phosphorus and nitrogen-containing oligomeric polyphosphoramide [133], (c) polyphosphoramids [134], (d) POCODA synthesized by phosphorus oxychloride and 4,4'-diaminodiphenyl ether [135], (e) hyperbranched carbon agent (CT) [136], (f) polyphosphoramide (DM-H) [137], (g) Si elements introduced into polyphosphateamides (DM-Si) [138], (h) polyphosphate flame retardant (PFRS) [139], (i) bio-based plant-derived diphenolic acid flame retardant [14], (j) electrostatically assembled product of CS and PA (CTS/PA) [142], and (k) core–shell bio-based flame retardant synthesized by chitosan microspheres and PA (Redrawn from reference [143] Copyright (2022) Elsevier)

Table 7. Typical flame retardant and mechanical property parameters of PLA/FR composites.

Year	Fillers	Types and mechanisms of FRs	Impact strength (GPa)	Young’s modulus (GPa)	Elongation at break (%)	Tensile Strength (MPa)	pHRR (kW/m^2)	THR (MJ/m^2)	UL-94	LOI (%)	TTI	FRI	Rank[#]	Ref
2018	3 wt% PPDA (Figure 8a)	P–N-based (C/G cases)	−20.0% (2.4 kJ·m^{-2}) *	-	−8.3% (3.3)	−8.8% (62.0)	−11.3%	−9.9%	V-0	25.5	72 (52)	2.0	Good; N	[132]
2020	3 wt% PPP (Figure 8b)	P–N-based (C/G cases)	-	-	−23.7% (10.3)	−8.5% (55.4)	+0.7%	−14.2%	V-0	32.5	48 (64)	0.7	Poor; N	[133]
2021	1 wt% PPDA-8 (Figure 8c)	P–N-based (C/G cases)	-	-	+2.3%	+11.0%	-	-	V-0	26.8	68 (64)	0.9	Poor; P	[134]
2021	2% POCODA+10% APP (Figure 8d)	P–N-based (C/G cases)	-	-	-	-	−21.7%	−22.1%	V-0	29.0	67 (79)	1.6	Good; -	[135]
2018	20 wt% APP/CT (4:1)+AHP (3:1) (Figure 8e)	P–N-based (C/G cases)	-	-	-	-	−87.5%	−46.5%	V-0	43.5	15 (32)	6.0	Good; -	[136]
2020	2 wt% DM-H (Figure 8f)	P–N-based (C/G cases)	−5.9% (3.2)	+1.3% (2.37)	+9.5% (10.4)	−3.8% (59.7)	−0.8%	-	V-0	29.7	-	-	-; P	[137]
2021	1.0 wt% DM-Si (Figure 8g)	P–N–Si-based (C/G cases)	maintain	maintain	+50.0%（10.8）	−2.4% (59.2)	−15.5%	−2.8%	V-0	27.9%	76 (69)	1.3	Good; P	[138]
2018	3.8 wt% PFRS + 11.2 wt% APP PFRS (Figure 8h)	P-based (C/G cases)	-	-	-	-	−46.0%	−40.4%	V-0	29.7	54 (68)	2.4	Good; -	[139]
2021	6 wt% PPD (Figure 8i)	Bio-based & P-based (C/G cases)	+31.0%（4.2）	-	-	+4.3%（57.5）	−6.9%	−4.4%	V-0	27.1	66 (71)	1.0	Good; P	[14]

2021	3% CTS/PA (Figure 8j)	Bio-based & Intumescent (C/G cases)	-	-	-	-	−19.1%	−26.2%	V-0	30.5	44 (40)	1.8	Good; -	[142]
2022	9 wt% PA@CHTM (Figure 8k)	Bio-based & Intumescent (C/G cases)	-	+90.9% （2.1）	−25.0% （3.3）	+0.5% （58.4）	−3.3%	−2.5%	V-0	29.6	17 (32)	0.6	Poor; P	[143]

Note: + indicates increasing and – indicates decreasing, ^The flame retardant mechanism exerted by FRs is represented by the C case (the condensed phase flame retardant mechanism) and the G case (the gas phase flame retardant mechanism), * the values in brackets are the specific performance data of the modified PLA material, poly (phenylphosphoryl phenylenediamine) (PPDA), phosphorus and nitrogen-containing oligomeric polyphosphoramide (PPP), polyphosphoramids (PPDA-8), the product synthesized by phosphorus oxychloride and 4,4’-diaminodiphenyl ether (POCODA), hyperbranched carbon agent (CT), polyphosphoramide synthesized by dimethyl methylphosphonate and 1,6-hexanediamine (DM-H), Si elements introduced into polyphosphateamides (DM-Si), polyphosphate flame retardant synthesized by bisphenolic acid-based monomer and phosphorus oxychloride (PFRS), plant-derived diphenolic acid flame retardant (PPD), electrostatically assembled product of CS and PA (CST/PA), and core–shell bio-based flame retardant synthesized by chitosan microspheres and PA (PA@CHTM), #The “Poor,” “Good,” or “Excellent” ranks are assessed for the cases based on the Flame Retardancy Index (FRI) results; P and N indicate the positive and negative effects of flame retardants on the mechanical properties of PLA composites, respectively.

3.5 Flame retardants with fibers and polymers

3.5.1. Flame retardants with fibers

P-containing FRs are essential because of their high efficiency, low loading, and less corrosive effect on the equipment during processing and combustion [15]. FRs with a high P content have a significant FR effect on PLA [144, 145]. Fibers can impart both good flame retardancy and good mechanical properties to PLA when combined with FRs. Selected representative findings are presented in **Figure 9**, and the corresponding mechanical properties and FR performance indices are summarized in **Table 8**.

Wool fiber (WF), a recycled protein-based natural animal fiber, possess inherent FR and antidripping capabilities during combustion owing to its rich N and S content. It exhibits a low HRR, high ignition temperature, and 25.2% LOI. It possesses a microfibrillated network structure that retains a high tensile strength. Amino acids and abundant S in WF catalyze dehydration and char layer production, limiting the possibility of melt dripping for PLA. Tawiah's group synthesized a new P-based FR phenylphosphonic 3(2-aminobenzo thiazole) (P-TAB) and combined it with recycled WF. The loading of 3 wt% P-TAB and 20 wt% WF in PLA achieved a UL-94 V-0 rating and a 28.5% LOI. The tensile strength increased by 26.6% with the same content of additives, and Young's modulus increased considerably **(Figure 9a)** [146].

Wood flour, an abundant and low-cost renewable natural fiber with a chemical structure similar to that of oxidized cellulose, improves the thermomechanical properties of common plastics. A composite obtained by mixing wood flour and APP with PLA/polyethylene glycol

(PEG) exhibited a denser carbon layer with 30.6% LOI and a 30.5% decrease in the pHRR. Besides, the final ternary composite changed from brittle to ductile with an elongation at the break increase of 92.1% [147].

Jute, a plant fiber, can be woven into high-strength rough filaments. Chemically modified jute fibers with DOPO derivatives (DOPO–maleic anhydride (MA)) were used to prepare FR PLA composites. Compared with the unmodified DOPO composite, the addition of 15% jute and 5% DOPO-MA resulted in an increased LOI value of PLA to 27.1% as well as a UL-94V-0 rating. The composite exhibited superior mechanical properties **(Figure 9b)** [148].

Glass fiber (GF), an inorganic nonmetallic material with a monofilament diameter typically below 20 microns, has strong heat resistance, corrosion resistance, and mechanical strength. It is used as polymer reinforcement material. APP and triphenyl phosphate, (TPP) selected as FRs, were blended with GF to form PLA/PC composites [149]. Various bio-based fibers have been developed and recycled in reinforced modified polymers in recent years owing to increasing concerns regarding the potential value of biomass waste. Zhan et al. found that PLA composites fabricated by incorporating 20% ramie fiber (RF) with 30% aluminum diethyl phosphinate (AlPi), melamine cyanurate, (MCA) and nanosilica (SiO_2)-based FR achieved UL-94 V-0 rating with an LOI value of 30.1%. The mechanical properties of the final material were not severely impaired because of the fiber reinforcement and high adhesion between FRs and the matrix [150].

Guadalupe et al. recovered keratin fibers (KFS) from tannery waste and combined them with traditional FRs to prepare PLA composites. Notably, the addition of 3 phr KFS and 30 phr aluminum hypophosphite to PLA gave a V-0 rating in the UL-94 test. It increased stiffness and Young’s modulus by 14.5% compared with that of pure PLA [151].

Hu et al. reported that interfacial nanoparticles could be compatibilized by using immiscible polymer blends. They synthesized a series of reactive nanoparticulate compatibilizers containing both epoxy groups and polymer chains for interface enhancement and the functionalization of polymer blends [152]. They placed boehmite nanorods at the PLA–Polypropylene (PP) interface through an in-situ reaction to improve compatibility (**Figure 9c**). The 7%-reactive nanorods increased the tensile strength and elongation at the break of the blends by 163% and 601%, respectively. Meanwhile, the pHRR decreased by 51.4% in the cone calorimetry test.

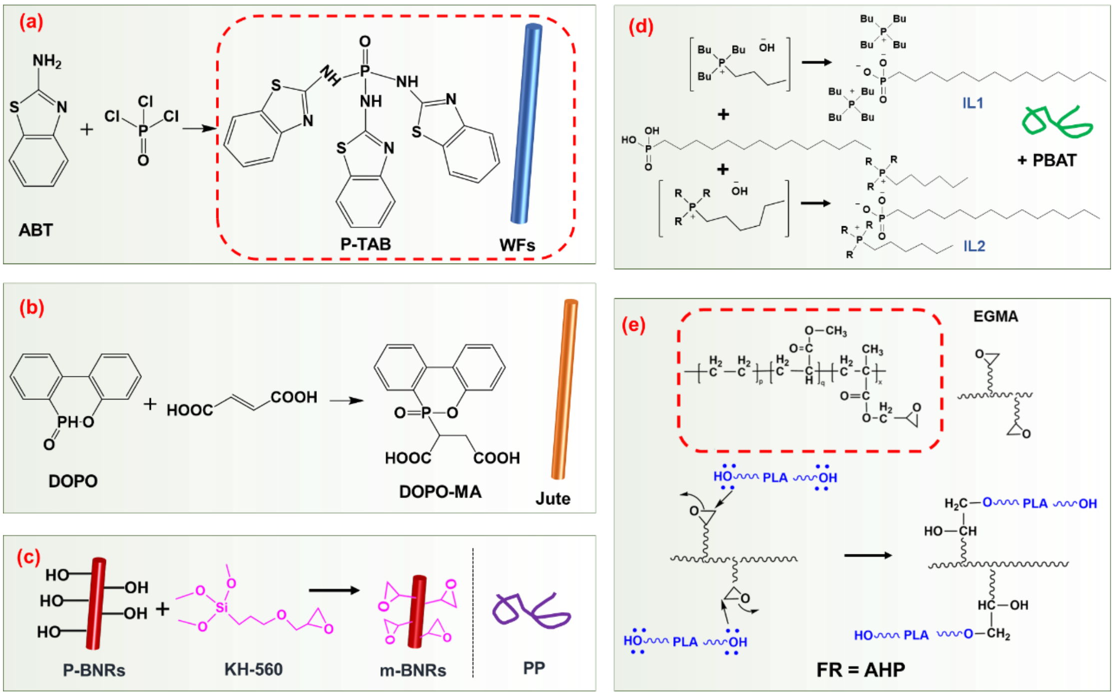

Figure 9. Schematic illustration for the preparation of (a) phenylphosphonic 3(2-aminobenzothiazole) (P-TAB) and Wool fiber (redrawn from reference [146]; copyright (2019) Express Polymer Letters), (b) DOPO derivatives (DOPO-MA) and jute fiber (redrawn from

reference [148]; copyright (2017) Elsevier), (c) Janus nanorods (redrawn from reference [152]; copyright (2021) Elsevier), and (d) ionic liquids (IL1, IL2) and polybutylene adipate terephthalate (PBAT)/PLA composites (redrawn from reference [153]; copyright (2021) Elsevier). (e) Possible reaction mechanism of PLA/ethylene-acrylic ester-glycidyl methacrylate terpolymer (EGMA) and blending with AHP (as a flame retardant) (redrawn from reference [154]; copyright (2017) ACS).

Table 8. Typical flame retardant and mechanical property parameters of PLA/fiber/FR composites.

Year	**Fillers**	**Types and mechanisms of FRs**	**Impact strength (GPa)**	**Young's modulus (GPa)**	**Elongation at break (%)**	**Tensile Strength (MPa)**	**pHRR (kW/m^2)**	**THR (MJ/m^2)**	**UL-94**	**LOI (%)**	**TTI**	**FRI**	**Rank**[#]	**Ref**
2019	3 wt% P-TAB+20 wt% WF (P–N-based) (Figure 9a)	P–N-based (C/G cases)	-	-	-	+26.6%	−25.9%	−42.8%	V0	28.5	40 (40)	2.4	Good; P	[146]
2019	10 wt% APP +10 wt% OWF	P–N-based (C/G cases)	-	-19.1 (1.8) *****	+92.1% (9.8)	−58.6% (27.8)	−30.8%	−21.8%	V0	30.6	55 (62)	1.1	Good; P	[147]
2017	5% DOPO-MA+15% jute (Figure 9b)	P-based (C/G cases)	-	-	-	-	−25.1%	-	V0	27.1	-	-	-; -	[148]
2019	30% GF+5% APP+5% TPP	P–N-based (C/G cases)	-	-	-	-	−73.9%	−35.4%	-	25.9	73 (70)	6.2	Good; -	[149]
2022	20% RF+30% FR (AlPi,MCA and SiO_2)+0.6% TGIC	P–N–Si-based & metal-containing (C/G cases)	-	-	-	-	−22.5%	−14.9%	V0	30.1	43 (31)	2.1	Good; -	[150]
2017	3 phr Keratin fiber+30 phr ATH	Metal-containing (C/G cases)	-	+14.5%	−27.4%	−18.7%	-		V0		-	-	-; N	[151]
2021	50 wt% aPP+7 wt% m-BNRs (Figure 9c)	Si-based (C/G cases)	-	-	+601.0% (9.5)	+163.0%	−51.4%	−2.2%	V-0	21.7	26（25）	2.1	Good; P	[152]

2021	20 wt% PBAT+0.7 wt% ILs (Figure 9d)	P-based (C/G cases)	-	-	+219.4% (281.1); +107.0% (182.6)	−42.3% (9.7); −36.3% (10.7)	-	-	-	28.1; 27.3	-	-	-; P	[153]
2017	20 wt% EGMA+20 wt% AHP (Figure 9e)	P-based & metal-containing (C/G cases)	11 times (22 kJ/m^2)	-	22 times	-	-68.2%	-8.1%	V-0	26.6	44 (50)	3.0	Good; P	[154]
2017	20 wt% PBS+5 wt% TCP	P-based (C/G cases)	+174.6% (3.5)	+9.5% (2.1)	+77.8% (3.2)	−14.4% (45.1)	-	-	V-2	27.0	-	-	-; P	[155]
2017	7% APP+14% PEG	P-based (C/G cases)	2 times	-	38 times	14 times	-10.7%	-4.5%	V-0	-	27 (32)	1.0	Good; P	[156]
2019	20 wt% GNR+18 wt% SiAHP	P–Si-based (C/G cases)	385% (13.1 kJ.m^{-2})		17 times (72.0)	−64.4% (24.5)	-69.8%	-28.2%	V-0	26.5	61 (47)	5.5	Good; P	[157]
2019	BUP+20 wt% APP	P-based (C/G cases)	15.9 times (15.9 kJ.m^{-2})	−31.0% (1.3)	13.7 times (107.1)	−58.1% (28.5)	−48.9%	−41.1%	V-0	27.0	66 (71)	3.1	Good; P	[158]
2019	10 wt% APP+1.5 wt% EG	P-based & C-based (C/G cases)	10.3 times (18.5 kJ.m^{-2})	−28.9% (1.4)	17.9 times (139.8)	−40.7% (40.3)	−39.2%	−37.0%	V-0	28.0	-	-	-; P	[159]

Note: + indicates increasing and –indicates decreasing, ^The flame retardant mechanism exerted by FRs is represented by the C case (the condensed phase flame retardant mechanism) and the G case (the gas phase flame retardant mechanism), *the values in brackets are the specific performance data of the modified PLA material, phenylphosphonic 3(2-aminobenzothiazole) comminated with recycled WF (P-TAB+WFs), Wood flour (OWF), jute fiber combined with DOPO derivatives (DOPO-MA + jute), Glass fiber (GF), triphenyl phosphate (TPP), ramie fiber (RF), 1,3,5-triglycidyl isocyanurate (TGIC), keratin fibers (KFS), aluminum trihydroxide (ATH), acrylic acid grafted PP (APP), surface-modified boehmite nanorods containing reactive epoxy (m-BNRs), polybutylene adipate terephthalate (PBAT), ionic liquids (ILs), ethylene-acrylic ester-glycidyl methacrylate terpolymer (EGMA), aluminum hypophosphite (AHP), poly (butylene succinate) (PBS), tricresyl phosphate (TCP), polyethylene glycol (PEG), NR-graft-glycidyl methacrylate (GNR), Si-modified aluminum hypophosphite (SiAHP), unsaturated polyester (BUP), and expandable graphite (EG). #The “Poor,” “Good,” or “Excellent” ranks are assessed for the cases based on the Flame Retardancy Index (FRI) results; P and N indicate the positive and negative effects of flame retardants on the mechanical properties of PLA composites, respectively.

3.5.2.FR and polymers

The above sections summarize the cases of adding FRs and fibrous fillers to balance the mechanical and flame retardancy properties of PLAs. PLA has also been used in combination with other polymers. Blending PLA with other flexible polymers is a simpler and more feasible method compared to copolymerization and plasticization. Previous studies combined PLA with biocompatible and biodegradable polymers such as starch, poly(hydroxybutyrate) (PHA) [160], poly (propyl carbonate) (PPC), poly (ε-caprolactone) (PCL) [161], and poly (butylene succinate) (PBS) [162, 163]. These blends increased the toughness of PLA without compromising its biodegradability.

Suparanon et al. blended PBS with PLA in a twin-screw extruder to enhance toughness followed by the addition of tricresyl phosphate (TCP) and montmorillonite (MMT) to improve the flame retardancy. The impact toughness of the PLA sample increased by approximately 144% to that of neat PLA with 20 wt% PBS. Compared to the PLA/TCP blend, the LOI index declined from 30.1% to 27.0% with the addition of PBS, achieving a V-2 rating in the UL-94 test [155]. Biodegradable PEG is also functions as a plasticizer and toughening agent for PLA. Sun et al. incorporated 7% APP and 14% PEG into PLA to achieve a V-0 rating in the UL-94 test and a 14% reduction in the pHRR in the cone calorimetry test. The elongation at break and impact strength of PLA composites are 38 and 2 times higher than those of pure PLA, respectively [156].

PBAT, a biothermoplastic with high toughness and good biodegradability, is often blended with PLA for processability enhancement and application. Compatibilizers, transesterification agents, and chain extenders were introduced to effectively reduce the interfacial tension and increase interfacial adhesion considering the mechanical properties of the composites to be adversely affected by the poor compatibility of PBAT and PLA. Zhou et al. found that ionic liquids (ILs) combine the features of polymer lubricants, FRs, and interface compatibilizers owing to their chemical stability, nonflammability, and low saturated vapor pressure. Therefore, ILs containing P-based cations and anions with different alkyl substitutions were designed to interact with PBAT/PLA composites. The elongations at break of the composites containing 0.4 wt% ILs were 329.9% and 168.5% higher than those of pristine PBAT/PLA composites. 0.7 wt% of ILs in the PBAT/PLA composites exhibited good flame retardancy and LOI values of 28.1% and 27.3%, respectively **(Figure 9d)** [153].

Apart from adding a compatibilizer as the third phase to improve the interfacial interaction between polymers, the blending of FR PLA with reactive polymer elastomers is an efficient method to enhance toughness. Li et al. confirmed that the reaction blending of PLA with ethylene-acrylic ester-glycidyl methacrylate terpolymer (EGMA) formed an effective interfacial layer through the reaction between the glycidyl ester group in the EGMA and carboxyl and hydroxyl groups in PLA. An 80/20 blend of PLA/EGMA 80/20 blend (STPLA) with high toughness was prepared **(Figure 9e)** [154]. STPLA/20AHP increased the elongation at break and notched Izod impact strength by approximately 22 and 11 times, respectively than those of pure PLA. AHP also imparted excellent FR properties to blend with 26.6% LOI 26.6% and an acceptable UL-94 V0 rating.

The incorporation of rubbery elastomers into PLA is a sensitive approach for obtaining rubber-toughened PLA. Natural rubber (NR) was grafted to obtain NR-graft-glycidyl methacrylate (GNR), followed by in-situ dynamic vulcanization to obtain a PLA/GNR thermoplastic vulcanizate with excellent toughness [157]. Li et al. prepared super tough polylactic acid (TPLA) via dynamic vulcanization and the interfacial compatibilization of a bio-based unsaturated polyester (BUP). The viscosity of the treated TPLA increased significantly. The crosslinking of BUP and its transesterification with the PLA matrix at high temperatures toughened the generated droplets during combustion, preventing the further spreading of the flame with the melt flow [158]. This team also incorporated EG into the above combination to further improve the comprehensive properties of the composites and reduce the FR content [159]. 10 wt% APP and 1.5% EG the LOI value of TPLA to 28% with acceptable V-0 rating in the UL-94 test; the elongation at break and the notched impact strength were 17.9 and 10.3 times more than those of pure PLA, respectively.

3.6 Chain extension or crosslinking with other FRs

Inducing in-situ reactions during the blending process (reactive extrusion) is a practical approach for further enhancing the toughening effect of elastomers on PLA blends. The introduction of compatibilizers such as MA, PLA graft-MA (PLA-g-MA), glycidyl methacrylate (GMA), and maleate and isocyanate compounds improved the interfacial adhesion between PLA and elastomers, enhancing the mechanical properties of blends. **Figure 10** shows representative findings for the introduction of reactive group-bearing additives into PLA. The relevant mechanical parameters and FR performance indices are summarized in **Table 9**.

3.6.1. Isocyanate group

Ma et al. selected PLLA/PCL blends and added APP and 4,40-methylenediphenyl diisocyanate (MDI) to obtain FR composites **(Figure 10a)**. MDI reacted with active hydrogen on the surface of APP and was grafted to APP via an in-situ reaction. This improved interfacial adhesion with the substrate and increased toughness [164]. The FR properties of composites were enhanced and the impact strength increased from 1.0 kJ/m^2 to 13.5 kJ/m^2 with an increase in the APP content. Li et al. used MDI, PEG, and glycerol to form crosslinked polyurethane (CPU) to obtain TPLA and synthesized a new type of bio-based P- and N-containing FR (PA-HDA) blended with TPLA **(Figure 10b)** [165]. The modified TPLA acquired the UL-94 V-0 rating at 5 wt% PA-HDA loading. The FR TPLA maintained good tensile toughness and impact toughness. The elongation at break and the notched impact strength were increased to 207.3% and 5.0 kJ/m^2, respectively. Worasak et al. used toluene diphenyl diisocyanate (TDI) as a compatibilizer for PBAT and PLA. They blended composites with triene phosphate (TCP) and triethyl citrate (TEC) as effective plasticizers and impact modifiers, respectively. Both the flame retardancy and impact properties of the composites were improved [166].

Physical blending, the most common method of PLA FR modification, introduces different additive FRs into the PLA matrix. However, the poor self-reactivity of PLA and its surface hydrophobicity has several disadvantages: poor compatibility, impaired mechanical properties, and low durability.

It has recently been reported that the copolymerization of monomers and reactive FRs is an effective method to solve these issues. Yu et al. synthesized a P-containing FR, P–polylactic acid (P-PLA), via a chain extension reaction of l-lactide and DOPO derivatives. Subsequently, P-PLA was melt-blended with pure PLA to eliminate poor compatibility. DOPO existed individually to produce an FR PLA composite (FR-PLA) with satisfactory mechanical properties **(Figure 10c)** [167]. 10 wt% P-PLA increased the LOI value of PLA to 27.8%, and the UL-94 rating reached V-1. The tensile strength of FR-PLA10 was suitable for most applications. Mincheva et al. also chose the high-efficiency FR DOPO to synthesize FR bioplastic polylactides via a covalent bond, as presented in **Figure 10d**. The catalytic ring-opening polymerization of L, L-lactide with a pre-synthesized DOPO-diamine initiator, and the extruded phosphorylated polylactic acid oligomer (DOPO-PLA) was subjected to a bulk chain-coupling reaction with hexamethylene diisocyanate (HDI). The finally obtained phosphorylated PLA exhibited superior flame retardancy and the pHRR and THR were significantly reduced by 35% and 36%, respectively [168].

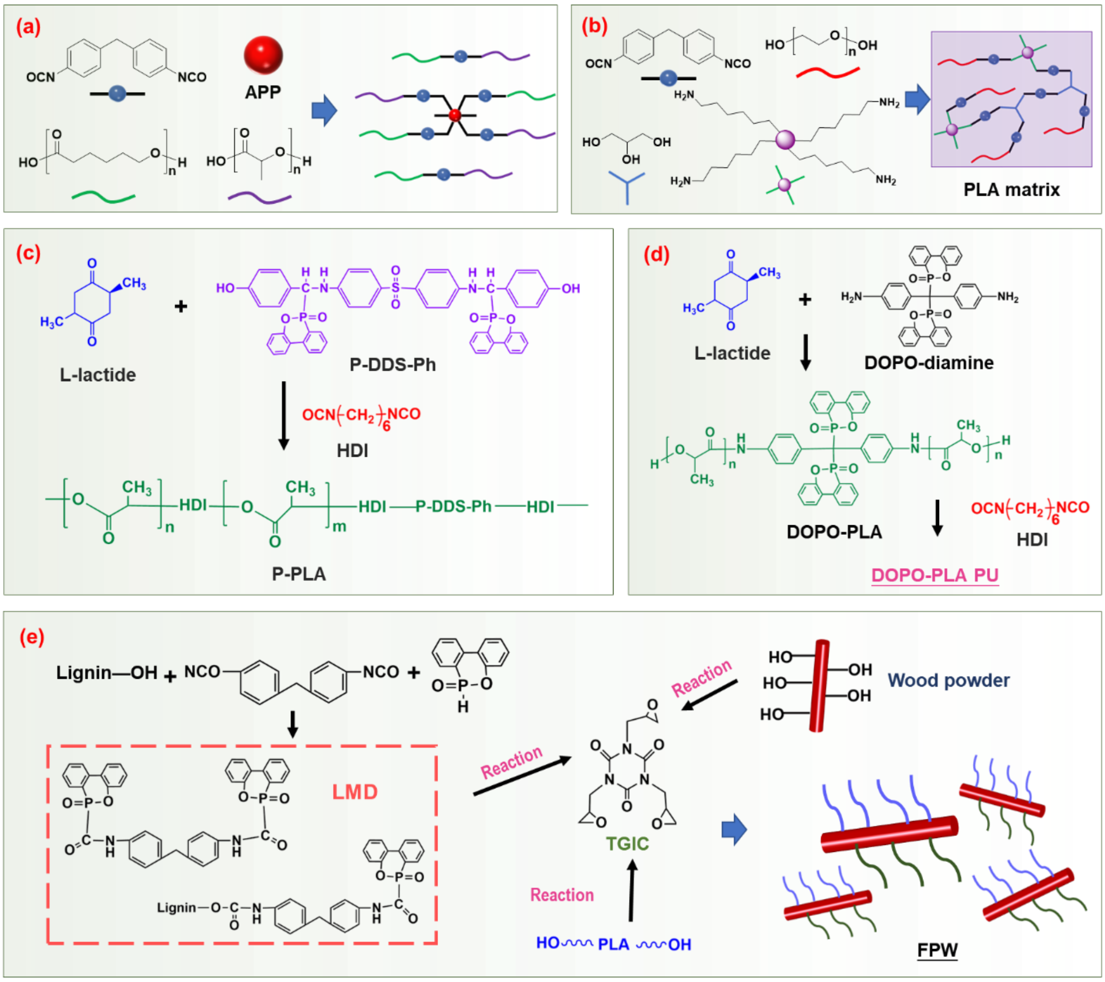

Figure 10. Schematic diagram of (a) the chemical reaction route of PLLA, PCL, and APP with 4,40-methylene diphenyl diisocyanate during melt blending (redrawn from reference [164]; copyright (2020) Wiley), (b) flame retardant and tough PLA by reactive blending (redrawn from reference [165]; copyright (2018) Elsevier), (c) chemical reaction route of phosphorus-containing PLA (redrawn from reference [167]; copyright (2018) Elsevier), (d) ring-opening polymerization for L, L-lactide with a pre-synthesized DOPO-diamine initiator (redrawn from reference [168]; copyright (2019) Wiley), and (e) the speculated blending mechanism of all-degradable flame retardant wood/PLA biocomposite with TGIC (redrawn from reference [169]; copyright (2020) Wiley).

Table 9. Typical flame retardant and mechanical properties parameters of PLA blend with other polymers.

Year	**Fillers**	**Types and mechanisms of FRs**	**Impact strength (GPa)**	**Young's modulus (GPa)**	**Elongation at break (%)**	**Tensile Strength (MPa)**	**pHRR (kW/m^2)**	**THR (MJ/m^2)**	**UL-94**	**LOI (%)**	**TTI**	**FRI**	**Rank[#]**	**Ref**
2020	18.1 wt% PCL+4.8 wt% MDI+4.8 wt% APP (Figure 10a)	P-based (C/G cases)	-	−33.4% (1.2) *	17.1 times (73.6)	−48.5% (33.2)	−2.5%	−7.4%	V-2	23.8	42 (44)	1.0	Good; P	[164]
2018	10 wt% PEG+2 wt% Gly+ 8 wt% MDI+5 wt% PA-HDA (Figure 10b)	P–N-based (C/G cases)	2.8 times (5.0 kJ/m^2)	-	26.6 times (207.3)	−12.2% (59.8)	-	-	V-0	26.0	-	-	-; P	[165]
2020	10 wt% PBAT+6 wt% TDI+20 wt% TCP+5 wt% TEC	P-based C/G cases)	-	+21.2% (2.7)	21.6 times (172.4)	+6.9% (32.7)	-	-	V-0	26.3	-	-	-; P	[166]
2018	10 wt% P-PLA (Figure 10c)	P-based (C/G cases)	-	-	-	−14.6% (61.8)	−18.7%	−35.3%	V-1	27.8	78 (66)	2.2	Good; N	[167]
2020	DOPO-PLA-PU (Figure 10d)	P-based (C/G cases)	-	-	-	-	−35.0%	−36.0%	V-0	-	16 (40)	0.9	Poor; -	[168]
2020	25% L15MD+4% TGIC (Figure 10e)	P-based (C/G cases)	26.1J m^{-1}	-	-	−10.9% (48.7)	-	-	V-0	28.6	-	-	-; P	[169]
2020	1.0 wt% PN+ 0.1 wt% TGIC	P–N-based (C/G cases)	-	+0.9% (3.4)	−19.0% (3.4)	+7.0% (76.0)	+2.2%	−5.8%	V-0	30.8	91 (79)	1.2	Good; P	[170]

Note: + indicates increasing and – indicates decreasing, ^The flame retardant mechanism exerted by FRs is represented by the C case (condensed phase flame retardant mechanism) and the G case (gas phase flame retardant mechanism), * the values in brackets are the specific performance data of the modified PLA material, PCL is poly (ε-caprolactone), MDI is 4,40-methylenediphenyl diisocyanate, PEG is polyethylene glycol, PA-HDA is P, N-containing FR derived from phytic acid and 1,6-hexanediamine, PBAT is polybutylene adipate terephthalate, TDI is toluenediphenyl diisocyanate, TCP is triene phosphate, TEC is triethyl citrate, P-PLA is phosphorus-containing flame-retardant PLA, DOPO-PLA-PU is the ring-opening polymerization product of L,L-lactide with a pre-synthesized DOPO-diamine initiator, LMD is a product reacted by lignin with DOPO, 4,4′-diphenylmethane diisocyanate, TGIC is triglycidyl isocyanurate, and PN is phosphorus–nitrogen flame retardant synthesized by using cytosine and diphenylphosphinic chloride, #The “Poor,” “Good,” or “Excellent” ranks are assessed for the cases based on the Flame Retardancy Index (FRI) results; P and N indicate the positive and negative effects of flame retardants on the mechanical properties of PLA composites, respectively.

3.6.2. Epoxy group

Triglycidyl isocyanurate (TGIC), a heterocyclic polyepoxide, is highly resistant to heat, weather, light, and corrosion. The epoxy groups of TGIC react with the terminal hydroxyl groups of PLA to elongate the chains or form crosslinked structures. Controlling the TGIC amount and the reaction time can have a favorable influence on the flame retardancy and mechanical properties of PLA composites [171]. In contrast to the conventional bulk mode, a fiber surface modification method was proposed by Wu et al. [172]. The tensile strength and modulus of PLA/sisal bio-based composites were enhanced as the interfacial adhesion was improved via in-situ reactive interfacial compatibilization with the addition of TGIC. Hu et al. prepared a P–N FR using cytosine and diphenylphosphinic chloride [170]. The PLA/0.5 wt% P–N composite achieved a UL-94 V-0 rating and an LOI value of 30.4%. Moreover, the tensile strength and elongation at the break of PLA/ P–N composite were restored to the original level to that of PLA when 0.1 wt% TGIC was introduced as a microcrosslinking agent.

Hu et al. reacted lignin with DOPO and MDI to prepare completely biodegradable wood-PLA biocomposites (FPW) (**Figure 10e**) [169]. The composite with 30 wt% of wood content, 4 wt% TGIC showed 28.6% LOI with an impact strength and tensile strength of 26.1 J m^{-1} and 48.7 MPa, respectively.

4. Concluding remarks and future perspectives

PLA, a common bio-based degradable polyester obtained from corn, potato, and cassava, is nontoxic, biodegradable, and biocompatible. It also has high mechanical strength and strong processing plasticity. Its mechanical properties are comparable to those of petroleum-based polymers such as polyethylene terephthalate. Moreover, it can be thoroughly degraded into small molecules (water and carbon dioxide) and is regarded as an ideal material for solving the solid waste disposal issue. It has received extensive attention from researchers. However, PLA has certain disadvantages as a bio-based polyester material: (1) The thermal stability and impact resistance of PLA are inferior to those of traditional thermoplastic polymers, giving rise to a narrow processing window; (2) It has a low LOI and is easily ignited to produce molten droplets, posing a fire risk; and (3) the PLA molecular chain is more sensitive to environmental factors, which cause aging and reduce its performance. Despite the promising prospects and imminent development demands of PLA, they require considerable modification.

Novel FR PLA systems have been systematically reviewed in recent years. The additives used are P- and C-based FRs. PLA is an aliphatic polyester. Hence, instead of producing crosslinked structures (carbon layer), its molecular chains break violently at high temperatures. The entire material rapidly burns without a barrier shielding layer when PLA is exposed to flame. It is conceivable that additives with better char-forming capacities (carbon-based, aromatic, and polyhydroxy) are beneficial for FR PLA polymers. Phosphate-based fillers are FRs with excellent compatibility with PLA. Phosphorus and oxygen radicals released by decomposition in the gas phase preferentially capture the active hydrogen and hydroxyl radicals during PLA pyrolysis to inhibit further cracking and combustion of the PLA backbone. In contrast, a series of low molecular weight phosphates form inorganic phosphates via self-crosslinking dehydration and promote the dehydration of the PLA backbone into char, assisting the condensed-phase FR. Nevertheless, the excellent catalytic decomposition ability of phosphorus-containing FRs inevitably decreases the thermal stability of PLA. The trend of the

TTI values obtained by cone calorimetry in the cases generally decreased, and the final calculated Flame Retardancy Index values range from 0.8 to 6.1, which rarely reached an excellent rank (above 10).

Therefore, we propose the following strategies and principles for the improvement of FR PLA:

i. The preparation of FRs or fillers should be simple, and the additive synthesis process should be free of toxic and hazardous waste generation.

ii. FRs and fillers should match the processing properties of the polymer matrix. This will ensure that no effect is exerted on the essential performance of the matrix during processing, preventing the premature decomposition of the polymer or side reactions. In addition, preparing FRs with high thermal stability (new carbonization catalysts, carbon formers, and foaming agents) is an essential aspect of the flame-retardancy enhancement of PLA.

iii. FRs are prone to stress concentration owing to their large particle size, which impairs the mechanical properties of the material. Consequently, the miniaturization of FRs is a vital part of FR technology.

iv. Efforts have been made to improve the mechanical properties of PLA by reinforcing FRs with fiber, reactive extrusion, and rubber toughening. However, toughness and mechanical strength result in the inverse performance of PLA and impair the original performance. Therefore, developing a comprehensive toughening strategy to obtain highly toughened PLA without reducing stiffness remains a big challenge.

With the growing awareness of environmental protection, there is an increasing demand for environmentally friendly FRs with high FR efficiency, nontoxicity, low cost, and good compatibility with polymers. The FR technology has made remarkable progress in ultrafine, microencapsulation, and macromolecular structural designs [173], reactive extrusion [174], surface modification of polymer FR materials, and synergistic compounding between FRs [26, 175]. The field of FRs has more vigorous and prosperous prospects with global progress in FR technology research.

The popularization of the concept of big data and the emergence of the human brain-computer combines research, analysis, the prediction of performance modification, and filler processing methods [176,177]. Many studies have guided the economical design of high-efficiency FRs. In the future, PLA needs to be explored further. Maximizing the value of materials will facilitate the transformation of ideas into actual academic output.

The environmental impact of materials is an essential guide for material design. considering the increasingly serious energy crisis, the research and development of synthetic materials must shift from petrochemical-based to bio-based materials. Bio-based PLA materials can avert the shortage of production resources and reduce pollution caused by waste products. Therefore, the exploration of two primary issues, preparing long-life, fast-degrading FR PLA composites and understanding the corresponding mechanism of action will be of great significance for environmental protection, sustainable development, and the realization of the actual needs of society.

Acknowledgment

The authors gratefully acknowledge financial support from the National Natural Science Foundation of China under Project numbers 22075010 and 22175017.

References

[1] M.J. Mochane, T.C. Mokhena, E.R. Sadiku, S.S. Ray, T.G. Mofokeng, Green Polymer Composites Based on Polylactic Acid (PLA) and Fibers, Green Biopolymers and their Nanocomposites 798 (2019) 29-54, https://doi.org/10.1007/978-981-13-8063-1_2.

[2] H. Vahabi, M. Shabanian, F. Aryanasab, R. Mangin, F. Laoutid, M.R. Saeb, Inclusion of modified lignocellulose and nano-hydroxyapatite in development of new bio-based adjuvant flame retardant for poly(lactic acid), Thermochimica Acta 666 (2018) 51-59, https://doi.org/https://doi.org/10.1016/j.tca.2018.06.004.

[3] S. Qiu, J. Sun, H. Li, X. Gu, B. Fei, S. Zhang, A green way to simultaneously enhance the mechanical, flame retardant and anti-ultraviolet aging properties of polylactide composites by the incorporation of tannic acid derivatives, Polym. Degrad. Stab. 196 (2022) 109831, https://doi.org/10.1016/j.polymdegradstab.2022.109831

[4] W. Niu, Y. Guo, W. Huang, L. Song, Z. Xiao, Y. Xie, Y. Wang, Aliphatic chains grafted cellulose nanocrystals with core-corona structures for efficient toughening of PLA composites, Carbohydr Polym 285 (2022) 119200, https://doi.org/10.1016/j.carbpol.2022.119200.

[5] X. Wang, W. Wang, S. Wang, Y. Yang, H. Li, J. Sun, X. Gu, S. Zhang, Self-intumescent polyelectrolyte for flame retardant poly (lactic acid) nonwovens, J Clean Prod 282 (2021) 124497, https://doi.org/10.1016/j.jclepro.2020.124497.

[6] M. Gelmont, M. Yuzefovitch, D. Yoffe, E. Eden, S. Levchik, Alkylation of Aromatic Compounds with Pentabromobenzyl Bromide and Tetrabromoxylene Dibromide as a New Route to High Molecular Weight Brominated Flame Retardants, Polymers (Basel) 12(2) (2020), https://doi.org/10.3390/polym12020352.

[7] M. Altarawneh, Temperature-dependent profiles of dioxin-like toxicants from combustion of brominated flame retardants, J Hazard Mater 422 (2022) 126879, https://doi.org/10.1016/j.jhazmat.2021.126879.

[8] S.D. Shaw, A. Blum, R. Weber, K. Kannan, D. Rich, D. Lucas, C.P. Koshland, D. Dobraca, S. Hanson, L.S. Birnbaum, halogenated flame retardants do the fire safety benefits justify the risks, Rev Environ Health 25(4) (2010) 261-306,

[9] H. Xu, L. Meng, X. Zhao, J. Chen, J. Lu, J.M. Chovelon, Y. Ji, Accelerated oxidation of the emerging brominated flame retardant tetrabromobisphenol S by unactivated peroxymonosulfate: The role of bromine catalysis and formation of disinfection byproducts, Water Res 204 (2021) 117584, https://doi.org/10.1016/j.watres.2021.117584.

[10] L. Costes, F. Laoutid, M. Aguedo, A. Richel, S. Brohez, C. Delvosalle, P. Dubois, Phosphorus and nitrogen derivatization as efficient route for improvement of lignin flame retardant action in PLA, Eur Polym J 84 (2016) 652-667, https://doi.org/10.1016/j.eurpolymj.2016.10.003.

[11] M. Maqsood, G. Seide, Biodegradable Flame Retardants for Biodegradable Polymer, Biomolecules 10(7) (2020) 1308, https://doi.org/10.3390/biom10071038.

[12] Z. Kovacevic, S. Flincec Grgac, S. Bischof, Progress in Biodegradable Flame Retardant Nano-Biocomposites, Polymers (Basel) 13(5) (2021)741, https://doi.org/10.3390/polym13050741.

[13] M.J. Sim, S.H. Cha, Efficient polymeric phosphorus flame retardant: flame retardancy, thermal property, and physical property on polylactide, Polymer Bulletin 76(7) (2018) 3463-3479, https://doi.org/10.1007/s00289-018-2558-9.

[14] S. Qiu, J. Sun, Y. Li, T. Zhu, H. Li, X. Gu, B. Fei, S. Zhang, Life cycle design of fully bio-based poly(lactic acid) composites with high flame retardancy, UV resistance, and degradation capacity, J Clean Prod 360 (2022) 132165, https://doi.org/10.1016/j.jclepro.2022.132165.

[15] B. Tawiah, B. Yu, B. Fei, Advances in Flame Retardant Poly(Lactic Acid), Polymers (Basel) 10(8) (2018), https://doi.org/10.3390/polym10080876.

[16] V.A. Yiga, M. Lubwama, S. Pagel, J. Benz, P.W. Olupot, C. Bonten, Flame retardancy and thermal stability of agricultural residue fiber-reinforced polylactic acid: A Review, Polym Composite 42(1) (2020) 15-44, https://doi.org/10.1002/pc.25835.

[17] G. Zhao, H.-Y. Liu, X. Cui, X. Du, H. Zhou, Y.-W. Mai, Y.-Y. Jia, W. Yan, Tensile properties of 3D-printed CNT-SGF reinforced PLA composites, Compos Sci Technol (2022) 109333, https://doi.org/10.1016/j.compscitech.2022.109333.

[18] P. Majgaonkar, R. Hanich, F. Malz, R. Brüll, Chemical Recycling of Post-Consumer PLA Waste for Sustainable Production of Ethyl Lactate, Chem. Eng. J. 423(1) (2021) 129952, https://doi.org/10.1016/j.cej.2021.129952.

[19] D.-D. Yang, C. Wu, G. Wu, S.-C. Chen, Y.-Z. Wang, Toughening of Polylactide with High Tensile Strength via Constructing an Integrative Physical Crosslinking Network Based on Ionic Interactions, Macromolecules 54(1) (2020) 291-301, https://doi.org/10.1021/acs.macromol.0c02181.

[20] Y. Xu, W. Zhang, Y. Qiu, M. Xu, B. Li, L. Liu, Preparation and mechanism study of a high efficiency bio-based flame retardant for simultaneously enhancing flame retardancy, toughness and crystallization rate of poly (lactic acid), Compos Part B-Eng 238(1) (2022) 109913, https://doi.org/10.1016/j.compositesb.2022.109913.

[21] H. Peltola, K. Immonen, L.S. Johansson, J. Virkajärvi, D. Sandquist, Influence of pulp bleaching and compatibilizer selection on performance of pulp fiber reinforced PLA biocomposites, J Appl Polym Sci 136(37) (2019) 47955, https://doi.org/10.1002/app.47955.

[22] E.M. Agaliotis, B.D. Ake-Concha, A. May-Pat, J.P. Morales-Arias, C. Bernal, A. Valadez-Gonzalez, P.J. Herrera-Franco, G. Proust, J.F. Koh-Dzul, J.G. Carrillo, E.A. Flores-Johnson, Tensile Behavior of 3D Printed Polylactic Acid (PLA) Based Composites Reinforced with Natural Fiber, Polymers (Basel) 14(19) (2022) 3976, https://doi.org/10.3390/polym14193976.

[23] H. Li, B. Liu, L. Ge, Y. Chen, H. Zheng, D. Fang, Mechanical performances of continuous carbon fiber reinforced PLA composites printed in vacuum, Compos Part B-Eng 225 (2021) 10277, https://doi.org/10.1016/j.compositesb.2021.109277.

[24] J.J. Wu, N. Gao, L. Jiang, G.J. Zhong, C. Deng, X. Gao, The coupling effect of cellulose nanocrystal and strong shear field achieved the strength and toughness balance of Polylactide, Int J Biol Macromol 207 (2022) 927-940, https://doi.org/10.1016/j.ijbiomac.2022.03.172.

[25] S. Qiu, Y. Li, P. Qi, D. Meng, J. Sun, H. Li, Z. Cui, X. Gu, S. Zhang, Improving the flame retardancy and accelerating the degradation of poly (lactic acid) in soil by introducing fully bio-based additives, Int. J. Biol. Macromol. 193 (2021) 44-52, https://doi.org/10.1016/j.ijbiomac.2021.10.119.

[26] Z. Zhou, J. Ma, K. Li, W. Zhang, K. Li, X. Tu, L. Liu, J. Xu, H. Zhang, A Plant Leaf-Mimetic Membrane with Controllable Gas Permeation for Efficient Preservation of Perishable Products, ACS Nano 15(5) (2021) 8742–8752, https://doi.org/10.1021/acsnano.1c00997.

[27] W.S. Chow, E.L. Teoh, J. Karger-Kocsis, Flame retarded poly(lactic acid): A review, Express Polym Lett 12(5) (2018) 396-417, https://doi.org/10.3144/expresspolymlett.2018.34.

[28] Y. Guo, S. He, X. Zuo, Y. Xue, Z. Chen, C.-C. Chang, E. Weil, M. Rafailovich, Incorporation of cellulose with adsorbed phosphates into poly (lactic acid) for enhanced mechanical and flame retardant properties, Polym. Degrad. Stab. 144 (2017) 24-32, https://doi.org/10.1016/j.polymdegradstab.2017.08.004.

[29] L. Costes, F. Laoutid, F. Khelifa, G. Rose, S. Brohez, C. Delvosalle, P. Dubois, Cellulose/phosphorus combinations for sustainable fire retarded polylactide, Eur Polym J 74 (2016) 218-228, https://doi.org/10.1016/j.eurpolymj.2015.11.030.

[30] G. Rajeshkumar, S. Arvindh Seshadri, G.L. Devnani, M.R. Sanjay, S. Siengchin, J. Prakash Maran, N.A. Al-Dhabi, P. Karuppiah, V.A. Mariadhas, N. Sivarajasekar, A. Ronaldo Anuf, Environment friendly, renewable and sustainable poly lactic acid (PLA) based natural fiber reinforced composites – A comprehensive review, J Clean Prod 310 (2021) 127483, https://doi.org/10.1016/j.jclepro.2021.127483.

[31] L.Q.N. Tran, C.A. Fuentes, C. Dupont-Gillain, A.W. Van Vuure, I. Verpoest, Understanding the interfacial compatibility and adhesion of natural coir fibre thermoplastic composites, Composites Science and Technology 80 (2013) 23-30, https://doi.org/https://doi.org/10.1016/j.compscitech.2013.03.004.

[32] B. Bax, J. Müssig, Impact and tensile properties of PLA/Cordenka and PLA/flax composites, Composites Science and Technology 68(7) (2008) 1601-1607, https://doi.org/https://doi.org/10.1016/j.compscitech.2008.01.004.

[33] A. Gholampour, T. Ozbakkaloglu, A review of natural fiber composites: properties, modification and processing techniques, characterization, applications, Journal of Materials Science 55(3) (2020) 829-892, https://doi.org/10.1007/s10853-019-03990-y.

[34] M. Jonoobi, J. Harun, A.P. Mathew, K. Oksman, Mechanical properties of cellulose nanofiber (CNF) reinforced polylactic acid (PLA) prepared by twin screw extrusion, Compos Sci Technol 70(12) (2010) 1742-1747, https://doi.org/10.1016/j.compscitech.2010.07.005.

[35] Z. Yang, X. Li, J. Si, Z. Cui, K. Peng, Morphological, Mechanical and Thermal Properties of Poly(lactic acid) (PLA)/Cellulose Nanofibrils (CNF) Composites Nanofiber for Tissue Engineering, Journal of Wuhan University of Technology-Mater. Sci. Ed. 34(1) (2019) 207-215, https://doi.org/10.1007/s11595-019-2037-7.

[36] S. Qian, K. Sheng, K. Yu, L. Xu, C.A. Fontanillo Lopez, Improved properties of PLA biocomposites toughened with bamboo cellulose nanowhiskers through silane modification, J Mater Sci 53(15) (2018) 10920-10932, https://doi.org/10.1007/s10853-018-2377-2.

[37] H. Yang, B. Shi, Y. Xue, Z. Ma, L. Liu, L. Liu, Y. Yu, Z. Zhang, P.K. Annamalai, P. Song, Molecularly Engineered Lignin-Derived Additives Enable Fire-Retardant, UV-Shielding, and Mechanically Strong Polylactide Biocomposites, Biomacromolecules 22(4) (2021) 1432–1444, https://doi.org/10.1021/acs.biomac.0c01656.

[38] J. Feng, Y. Sun, P. Song, W. Lei, Q. Wu, L. Liu, Y. Yu, H. Wang, Fire-Resistant, Strong, and Green Polymer Nanocomposites Based on Poly(lactic acid) and Core–Shell Nanofibrous Flame

Retardants, ACS Sustain. Chem. Eng 5(9) (2017) 7894-7904, https://doi.org/10.1021/acssuschemeng.7b01430.

[39] L. Zhang, Z. Li, Y.-T. Pan, A.P. Yáñez, S. Hu, X.-Q. Zhang, R. Wang, D.-Y. Wang, Polydopamine induced natural fiber surface functionalization: a way towards flame retardancy of flax/poly(lactic acid) biocomposites, Composites Part B: Engineering 154 (2018) 56-63, https://doi.org/https://doi.org/10.1016/j.compositesb.2018.07.037.

[40] X. Jin, E. Xiang, R. Zhang, D. Qin, M. Jiang, Z. Jiang, Halloysite nanotubes immobilized by chitosan/tannic acid complex as a green flame retardant for bamboo fiber/poly(lactic acid) composites, J Appl Polym Sci 138(1) (2020) 49621, https://doi.org/10.1002/app.49621.

[41] Y.-Y. Wang, Y.-F. Shih, Flame-retardant recycled bamboo chopstick fiber-reinforced poly(lactic acid) green composites via multifunctional additive system, Journal of the Taiwan Institute of Chemical Engineers 65 (2016) 452-458, https://doi.org/https://doi.org/10.1016/j.jtice.2016.05.010.

[42] D. Battegazzore, A. Frache, F. Carosio, Layer-by-Layer nanostructured interphase produces mechanically strong and flame retardant bio-composites, Composites Part B: Engineering 200 (2020) 108310, https://doi.org/https://doi.org/10.1016/j.compositesb.2020.108310.

[43] P. Jiang, S. Zhang, S. Bourbigot, Z. Chen, S. Duquesne, M. Casetta, Surface grafting of sepiolite with a phosphaphenanthrene derivative and its flame-retardant mechanism on PLA nanocomposites, Polymer Degradation and Stability 165 (2019) 68-79, https://doi.org/https://doi.org/10.1016/j.polymdegradstab.2019.04.012.

[44] K. Decsov, V. Takács, G. Marosi, K. Bocz, Microfibrous cyclodextrin boosts flame retardancy of poly(lactic acid), Polymer Degradation and Stability 191 (2021) 109655, https://doi.org/10.1016/j.polymdegradstab.2021.109655.

[45] Z. Xiong, Y. Zhang, X. Du, P. Song, Z. Fang, Green and Scalable Fabrication of Core–Shell Biobased Flame Retardants for Reducing Flammability of Polylactic Acid, ACS Sustain. Chem. Eng 7(9) (2019) 8954-8963, https://doi.org/10.1021/acssuschemeng.9b01016.

[46] S. Lee, D. Seong, Y. Ju, H.W. Kwak, W.S. Kim, D. Lee, Revealing the flame retardancy mechanism of highly transparent cellulose nanopapers fabricated by vacuum filtration assisted layer-by-layer deposition, Carbohydr. Polym. 246 (2020) 116628, https://doi.org/10.1016/j.carbpol.2020.116628.

[47] Y.-W. Jia, X. Zhao, T. Fu, D.-F. Li, Y. Guo, X.-L. Wang, Y.-Z. Wang, Synergy effect between quaternary phosphonium ionic liquid and ammonium polyphosphate toward flame retardant PLA with improved toughness, Compos Part B-Eng 197 (2020) 108192, https://doi.org/10.1016/j.compositesb.2020.108192.

[48] X. Shi, X. Peng, J. Zhu, G. Lin, T. Kuang, Synthesis of DOPO-HQ-functionalized graphene oxide as a novel and efficient flame retardant and its application on polylactic acid: Thermal property, flame retardancy, and mechanical performance, J Colloid Interface Sci 524 (2018) 267-278, https://doi.org/10.1016/j.jcis.2018.04.016.

[49] Y. Chen, M. Pan, Y. Li, J.-Z. Xu, G.-J. Zhong, X. Ji, Z. Yan, Z.-M. Li, Core-shell nanoparticles toughened polylactide with excellent transparency and stiffness-toughness balance, Compos Sci Technol 164 (2018) 168-177, https://doi.org/10.1016/j.compscitech.2018.04.037.

[50] A.N. Frone, M. Ghiurea, C.A. Nicolae, A.R. Gabor, S. Badila, D.M. Panaitescu, Poly(lactic acid)/Poly(3-hydroxybutyrate) Biocomposites with Differently Treated Cellulose Fibers, Molecules 27(8) (2022) 2390, https://doi.org/10.3390/molecules27082390.

[51] X. Jin, S. Cui, S. Sun, X. Gu, H. Li, J. Sun, S. Zhang, S. Bourbigot, The Preparation of an Intumescent Flame Retardant by Ion Exchange and Its Application in Polylactic Acid, ACS Applied Polymer Materials 1(4) (2019) 755-764, https://doi.org/10.1021/acsapm.8b00278.

[52] Q. Wu, X. Cui, C. Mu, J. Sun, X. Gu, H. Li, S. Zhang, Toward a new approach to synchronously improve the fire performance and toughness of polylactic acid by the incorporation of facilely synthesized ammonium polyphosphate derivatives, Compos Part A-Appl S 150 (2021) 106595, https://doi.org/10.1016/j.compositesa.2021.106595.

[53] G. Ran, X. Liu, J. Guo, J. Sun, H. Li, X. Gu, S. Zhang, Improving the flame retardancy and water resistance of polylactic acid by introducing polyborosiloxane microencapsulated ammonium polyphosphate, Compos Part B-Eng 173(15) (2019) 106772, https://doi.org/10.1016/j.compositesb.2019.04.033.

[54] X.D. Jin, S.P. Cui, S.B. Sun, X.Y. Gu, H.F. Li, X.D. Liu, W.F. Tang, J. Sun, S. Bourbigot, S. Zhang, The preparation of a bio-polyelectrolytes based core-shell structure and its application in flame retardant polylactic acid composites, Compos Part A-Appl S 124 (2019) 105485, https://doi.org/10.1016/j.compositesa.2019.105485.

[55] X. Zhao, L. Chen, D.-F. Li, T. Fu, L. He, X.-L. Wang, Y.-Z. Wang, Biomimetic construction peanut-leaf structure on ammonium polyphosphate surface: Improving its compatibility with poly(lactic acid) and flame-retardant efficiency simultaneously, Chemical Engineering Journal 412 (2021) 128737, https://doi.org/https://doi.org/10.1016/j.cej.2021.128737.

[56] Y. Zhang, Z. Xiong, H. Ge, L. Ni, T. Zhang, S. Huo, P. Song, Z. Fang, Core–Shell Bioderived Flame Retardants Based on Chitosan/Alginate Coated Ammonia Polyphosphate for Enhancing Flame Retardancy of Polylactic Acid, ACS Sustain. Chem. Eng 8(16) (2020) 6402-6412, https://doi.org/10.1021/acssuschemeng.0c00634.

[57] J. Jing, Y. Zhang, Z.-P. Fang, D.-Y. Wang, Core-shell flame retardant/graphene oxide hybrid：a self-assembly strategy towards reducing fire hazard and improving toughness of polylactic acid, Compos Sci Technol 165 (2018) 161-167, https://doi.org/10.1016/j.compscitech.2018.06.024.

[58] W. Yin, L. Chen, F. Lu, P. Song, J. Dai, L. Meng, Mechanically Robust, Flame-Retardant Poly(lactic acid) Biocomposites via Combining Cellulose Nanofibers and Ammonium Polyphosphate, ACS Omega 3(5) (2018) 5615-5626, https://doi.org/10.1021/acsomega.8b00540.

[59] X. Xu, J. Dai, Z. Ma, L. Liu, X. Zhang, H. Liu, L.-C. Tang, G. Huang, H. Wang, P. Song, Manipulating interphase reactions for mechanically robust, flame-retardant and sustainable polylactide biocomposites, Composites Part B: Engineering 190 (2020) 107930, https://doi.org/10.1016/j.compositesb.2020.107930.

[60] S. Ding, P. Liu, S. Zhang, Y. Ding, F. Wang, C. Gao, M. Yang, Preparation and characterization of cyclodextrin microencapsulated ammonium polyphosphate and its application in flame retardant polypropylene, J Appl Polym Sci 137(34) (2020) 49001, https://doi.org/10.1002/app.49001.

[61] G. Moradkhani, M. Fasihi, L. Brison, F. Laoutid, H. Vahabi, M.R. Saeb, Flame retardancy effect of phosphorus graphite nanoplatelets on ethylene-vinyl acetate copolymer: Physical blending versus chemical modification, Polym Advan Technol 32(11) (2021) 4296-4305, https://doi.org/10.1002/pat.5432.

[62] W. Yang, H. Zhang, X. Hu, Y. Liu, S. Zhang, C. Xie, Self-assembled bio-derived microporous nanosheet from phytic acid as efficient intumescent flame retardant for polylactide, Polymer

Degradation and Stability 191 (2021) 109664, https://doi.org/https://doi.org/10.1016/j.polymdegradstab.2021.109664.

[63] Y. Guo, K. Yang, X. Zuo, Y. Xue, C. Marmorat, Y. Liu, C.-C. Chang, M.H. Rafailovich, Effects of clay platelets and natural nanotubes on mechanical properties and gas permeability of Poly (lactic acid) nanocomposites, Polymer 83 (2016) 246-259, https://doi.org/10.1016/j.polymer.2015.12.012.

[64] K. Sirisinha, S. Wirasate, C. Sirisinha, N. Wattanakrai, One-Pot Reactive Melt Recycling of PLA Post-Consumer Waste for the Production of Block Copolymer Nanocomposites of High Strength and Ductility, Polymers 14(17) (2022) 3642, https://doi.org/10.3390/polym14173642.

[65] L. Zhu, J. Qiu, W. Liu, E. Sakai, Mechanical and thermal properties of rice Straw/PLA modified by nano Attapulgite/PLA interfacial layer, Compos. Commun. 13 (2019) 18-21, https://doi.org/10.1016/j.coco.2019.02.001.

[66] W. Cai, B. Wang, L. Liu, X. Zhou, F. Chu, J. Zhan, Y. Hu, Y. Kan, X. Wang, An operable platform towards functionalization of chemically inert boron nitride nanosheets for flame retardancy and toxic gas suppression of thermoplastic polyurethane, Compos Part B-Eng 178(1) (2019) 107462, https://doi.org/10.1016/j.compositesb.2019.107462.

[67] M. Dong, H. Zhang, L. Tzounis, G. Santagiuliana, E. Bilotti, D.G. Papageorgiou, Multifunctional epoxy nanocomposites reinforced by two-dimensional materials: A review, Carbon 185 (2021) 57-81, https://doi.org/10.1016/j.carbon.2021.09.009.

[68] S. He, Y.-Y. Gao, Z.-Y. Zhao, S.-C. Huang, Z.-X. Chen, C. Deng, Y.-Z. Wang, Fully Bio-Based Phytic Acid–Basic Amino Acid Salt for Flame-Retardant Polypropylene, ACS Appl Polym Mater 3(3) (2021) 1488-1498, https://doi.org/10.1021/acsapm.0c01356.

[69] W. Zhu, M. Yang, H. Huang, Z. Dai, B. Cheng, S. Hao, A phytic acid-based chelating coordination embedding structure of phosphorus–boron–nitride synergistic flame retardant to enhance durability and flame retardancy of cotton, Cellulose 27(8) (2020) 4817-4829, https://doi.org/10.1007/s10570-020-03063-3.

[70] C.V.S. Rosely, A.M. Joseph, A. Leuteritz, E.B. Gowd, Phytic Acid Modified Boron Nitride Nanosheets as Sustainable Multifunctional Nanofillers for Enhanced Properties of Poly(l-lactide), ACS Sustain. Chem. Eng 8(4) (2020) 1868-1878, https://doi.org/10.1021/acssuschemeng.9b06158.

[71] W. Yang, H. Zhang, X. Hu, Y. Liu, S. Zhang, C. Xie, Self-assembled bio-derived microporous nanosheet from phytic acid as efficient intumescent flame retardant for polylactide, Polym. Degrad. Stab. 191 (2021) 109664, https://doi.org/10.1016/j.polymdegradstab.2021.109664.

[72] K. Zhang, J. Li, L. He, Q. Guan, X. Xu, R. Miao, M. Wang, H. Zhou, Investigation on guanidine phosphate modified LDH and its flame-retardant mechanism in cellulosic composites, Applied Clay Science 228 (2022) 106646, https://doi.org/10.1016/j.clay.2022.106646.

[73] K. Zhou, K. Gong, F. Gao, L. Yin, Facile strategy to synthesize MXene@LDH nanohybrids for boosting the flame retardancy and smoke suppression properties of epoxy, Compos Part A-Appl S 157 (2022) 106912, https://doi.org/10.1016/j.compositesa.2022.106912.

[74] Y. Liu, X. Hu, S. Han, Y. Wang, Z. Wu, L. Qian, The fabrication of phytate and LDH-based hybrid nanosheet towards improved fire safety properties and superior smoke suppression of intumescent flame retardant LDPE, Thermochim Acta 714 (2022) 179271, https://doi.org/10.1016/j.tca.2022.179271.

[75] Y. Liu, Y. Gao, Z. Zhang, Q. Wang, Preparation of ammonium polyphosphate and dye co-intercalated LDH/polypropylene composites with enhanced flame retardant and UV resistance properties, Chemosphere 277 (2021) 130370, https://doi.org/10.1016/j.chemosphere.2021.130370.

[76] S. Zhang, Y. Yan, W. Wang, X. Gu, H. Li, J. Li, J. Sun, Intercalation of phosphotungstic acid into layered double hydroxides by reconstruction method and its application in intumescent flame retardant poly (lactic acid) composites, Polym. Degrad. Stab. 147 (2018) 142-150, https://doi.org/10.1016/j.polymdegradstab.2017.12.004.

[77] Z. Wei, C. Cai, Y. Huang, P. Wang, J. Song, L. Deng, Y. Fu, Eco-friendly strategy to a dual-2D graphene-derived complex for poly (lactic acid) with exceptional smoke suppression and low CO2 production, J Clean Prod 280(2) (2021) 124433, https://doi.org/10.1016/j.jclepro.2020.124433.

[78] L. Jia, W. Zhang, B. Tong, R. Yang, Crystallization, flame-retardant, and mechanical behaviors of poly(lactic acid)\9,10-dihydro-9-oxa-10-phosphaphenanthrene-10-oxide–calcium montmorillonite nanocomposite, Journal of Applied Polymer Science 136(3) (2019) 46982, https://doi.org/https://doi.org/10.1002/app.46982.

[79] T. Tang, S. Wang, Y. Jiang, Z. Xu, Y. Chen, T. Peng, F. Khan, J. Feng, P. Song, Y. Zhao, Flexible and flame-retarding phosphorylated MXene/polypropylene composites for efficient electromagnetic interference shielding, J Mater Sci Technol 111 (2022) 66-75, https://doi.org/10.1016/j.jmst.2021.08.091.

[80] H. Huang, D. Dong, W. Li, X. Zhang, L. Zhang, Y. Chen, X. Sheng, X. Lu, Synergistic effect of MXene on the flame retardancy and thermal degradation of intumescent flame retardant biodegradable poly (lactic acid) composites, Chinese J Chem Eng 28(7) (2020) 1981-1993, https://doi.org/10.1016/j.cjche.2020.04.014.

[81] M. Wang, G. Xiao, C. Chen, Z. Yang, F. Zhong, C. Chen, R. Zou, Y. Li, R. Li, Combining layered double hydroxides and carbon nanotubes to synergistically enhance the flame retardant properties of composite coatings, Colloid Surface A 638(5) (2022) 128315, https://doi.org/10.1016/j.colsurfa.2022.128315.

[82] W. Cai, Z. Li, T. Cui, X. Feng, L. Song, Y. Hu, X. Wang, Self-assembly of hierarchical MXene@SnO2 nanostructure for enhancing the flame retardancy, solar de-icing, and mechanical property of polyurethane resin, Compos Part B-Eng 244 (2022) 110204, https://doi.org/10.1016/j.compositesb.2022.110204.

[83] Y. Shi, Z. Wang, C. Liu, H. Wang, J. Guo, L. Fu, Y. Feng, L. Wang, F. Yang, M. Liu, Engineering titanium carbide ultra-thin nanosheets for enhanced fire safety of intumescent flame retardant polylactic acid, Compos Part B-Eng 236(1) (2022) 109792, https://doi.org/10.1016/j.compositesb.2022.109792.

[84] Y. Xue, J. Feng, S. Huo, P. Song, B. Yu, L. Liu, H. Wang, Polyphosphoramide-intercalated MXene for simultaneously enhancing thermal stability, flame retardancy and mechanical properties of polylactide, Chem. Eng. J. 397 (2020) 125336, https://doi.org/10.1016/j.cej.2020.125336.

[85] W. Chen, P. Liu, L. Min, Y. Zhou, Y. Liu, Q. Wang, W. Duan, Non-covalently Functionalized Graphene Oxide-Based Coating to Enhance Thermal Stability and Flame Retardancy of PVA Film, Nanomicro Lett 10(3) (2018) 39, https://doi.org/10.1007/s40820-018-0190-8.

[86] Y. Yu, Y. Zhang, L. Xi, Z. Zhao, S. Huo, G. Huang, Z. Fang, P. Song, Interface nanoengineering of a core-shell structured biobased fire retardant for fire-retarding polylactide with enhanced

toughness and UV protection, J Clean Prod 15 (2022) 130372, https://doi.org/10.1016/j.jclepro.2022.130372.

[87] F. Fang, S. Ran, Z. Fang, P. Song, H. Wang, Improved flame resistance and thermo-mechanical properties of epoxy resin nanocomposites from functionalized graphene oxide via self-assembly in water, Compos Part B-Eng 165 (2019) 406-416, https://doi.org/10.1016/j.compositesb.2019.01.086.

[88] W. Chen, P. Liu, Y. Liu, Q. Wang, W. Duan, A temperature-induced conductive coating via layer-by-layer assembly of functionalized graphene oxide and carbon nanotubes for a flexible, adjustable response time flame sensor, Chem. Eng. J. 353 (2018) 115-125, https://doi.org/10.1016/j.cej.2018.07.110.

[89] Y. Yuan, Y.T. Pan, Z. Zhang, W. Zhang, X. Li, R. Yang, Nickle nanocrystals decorated on graphitic nanotubes with broad channels for fire hazard reduction of epoxy resin, J Hazard Mater 402 (2021) 123880, https://doi.org/10.1016/j.jhazmat.2020.123880.

[90] X.Z. Wu, Y.R. Yao, M.M. Chen, H.R. Tian, J. Xiao, Y.Y. Xu, M.S. Lin, L. Abella, C.B. Tian, C.L. Gao, Q. Zhang, S.Y. Xie, R.B. Huang, L.S. Zheng, Formation of Curvature Subunit of Carbon in Combustion, J Am Chem Soc 138(30) (2016) 9629-33, https://doi.org/10.1021/jacs.6b04898.

[91] Y. Pan, Z. Guo, S. Ran, Z. Fang, Influence of fullerenes on the thermal and flame-retardant properties of polymeric materials, J Appl Polym Sci 137(1) (2019) 47538, https://doi.org/10.1002/app.47538.

[92] L. Xia, Y. Lv, Z. Miao, L. Luo, W. Luo, Y. Xu, C. Yuan, B. Zeng, L. Dai, A flame retardant fabric nanocoating based on nanocarbon black particles@polymer composite and its fire-alarm application, Chem. Eng. J. 433(2) (2022) 133501, https://doi.org/10.1016/j.cej.2021.133501.

[93] W. Yu, L. Sisi, Y. Haiyan, L. Jie, Progress in the functional modification of graphene/graphene oxide: a review, RSC Adv 10(26) (2020) 15328-15345, https://doi.org/10.1039/d0ra01068e.

[94] Y. Jiang, Z. Li, Preparation and characterization of a novel polyurethane/polyurethane modified graphene oxide composites, Colloid Polym Sci 299(11) (2021) 1767-1776, https://doi.org/10.1007/s00396-021-04879-6.

[95] B. Xue, T. Xu, D. Li, J. Xu, Y. Li, F. Wang, J. Zhu, A Pickering emulsion of a bifunctional interface prepared from Pd nanoparticles supported on silicane-modified graphene oxide: an efficient catalyst for water-mediated catalytic hydrogenation, Catal Sci Technol 10(4) (2020) 1096-1105, https://doi.org/10.1039/c9cy02002k.

[96] P. Yang, H. Wu, F. Yang, J. Yang, R. Wang, Z. Zhu, A Novel Self-Assembled Graphene-Based Flame Retardant: Synthesis and Flame Retardant Performance in PLA, Polymers (Basel) 13(23) (2021) 4216, https://doi.org/10.3390/polym13234216.

[97] S. Ran, F. Fang, Z. Guo, P. Song, Y. Cai, Z. Fang, H. Wang, Synthesis of decorated graphene with P, N-containing compounds and its flame retardancy and smoke suppression effects on polylactic acid, Compos Part B-Eng 170 (2019) 41-50, https://doi.org/10.1016/j.compositesb.2019.04.037.

[98] B. Tawiah, B. Yu, R.K.K. Yuen, Y. Hu, R. Wei, J.H. Xin, B. Fei, Highly efficient flame retardant and smoke suppression mechanism of boron modified graphene Oxide/Poly(Lactic acid) nanocomposites, Carbon 150 (2019) 8-20, https://doi.org/10.1016/j.carbon.2019.05.002.

[99] C. Guo, F. Xin, C. Zhai, Y. Chen, Flammability and thermal properties of modified carbon nanotubes in poly(lactic acid), J Thermoplast Compos 32(8) (2019) 1107-1122, https://doi.org/10.1177/0892705718785678.

[100] L. Gu, J. Qiu, Y. Yao, E. Sakai, L. Yang, Functionalized MWCNTs modified flame retardant PLA nanocomposites and cold rolling process for improving mechanical properties, Compos Sci Technol 161 (2018) 39-49, https://doi.org/10.1016/j.compscitech.2018.03.033.

[101] L. Zhang, W. Chai, W. Li, K. Semple, N. Yin, W. Zhang, C. Dai, Intumescent-Grafted Bamboo Charcoal: A Natural Nontoxic Fire-Retardant Filler for Polylactic Acid (PLA) Composites, ACS Omega 6(41) (2021) 26990-27006, https://doi.org/10.1021/acsomega.1c03393.

[102] W. Yang, B. Tawiah, C. Yu, Y.-F. Qian, L.-L. Wang, A.C.-Y. Yuen, S.-E. Zhu, E.-Z. Hu, T.B.-Y. Chen, B. Yu, H.-D. Lu, G.H. Yeoh, X. Wang, L. Song, Y. Hu, Manufacturing, mechanical and flame retardant properties of poly(lactic acid) biocomposites based on calcium magnesium phytate and carbon nanotubes, Compos Part A-Appl S 110 (2018) 227-236, https://doi.org/10.1016/j.compositesa.2018.04.027.

[103] X. Wen, Z. Liu, Z. Li, J. Zhang, D.-Y. Wang, K. Szymańska, X. Chen, E. Mijowska, T. Tang, Constructing multifunctional nanofiller with reactive interface in PLA/CB-g-DOPO composites for simultaneously improving flame retardancy, electrical conductivity and mechanical properties, Compos Sci Technol 188 (2020) 107988, https://doi.org/10.1016/j.compscitech.2019.107988.

[104] X. Cao, X. Chi, X. Deng, T. Liu, B. Yu, B. Wang, A.C.Y. Yuen, W. Wu, R.K.Y. Li, Synergistic effect of flame retardants and graphitic carbon nitride on flame retardancy of polylactide composites, Polym Advan Technol 31(7) (2020) 1661-1670, https://doi.org/10.1002/pat.4894.

[105] M. Zhang, X. Shi, X. Dai, C. Huo, J. Xie, X. Li, X. Wang, Improving the crystallization and fire resistance of poly(lactic acid) with nano-ZIF-8@GO, J Mater Sci 53(9) (2018) 7083-7093, https://doi.org/10.1007/s10853-018-2049-2.

[106] D. Wang, Y. Wang, X. Zhang, T. Li, M. Du, M. Chen, W. Dong, Preferred zinc-modified melamine phytate for the flame retardant polylactide with limited smoke release, New J Chem 45(30) (2021) 13329-13339, https://doi.org/10.1039/d1nj02219a.

[107] L. Xu, X. Wu, L. Li, Y. Chen, Synthesis of a novel polyphosphazene/triazine bi-group flame retardant in situ doping nano zinc oxide and its application in poly (lactic acid) resin, Polymers for Advanced Technologies 30(6) (2019) 1375-1385, https://doi.org/https://doi.org/10.1002/pat.4570.

[108] Y. Cao, Y. Ju, F. Liao, X. Jin, X. Dai, J. Li, X. Wang, Improving the flame retardancy and mechanical properties of poly(lactic acid) with a novel nanorod-shaped hybrid flame retardant, RSC Advances 6(18) (2016) 14852-14858, https://doi.org/10.1039/c5ra25112e.

[109] Y. Zhan, X. Wu, S. Wang, B. Yuan, Q. Fang, S. Shang, C. Cao, G. Chen, Synthesis of a bio-based flame retardant via a facile strategy and its synergistic effect with ammonium polyphosphate on the flame retardancy of polylactic acid, Polymer Degradation and Stability 191 (2021) 109684, https://doi.org/https://doi.org/10.1016/j.polymdegradstab.2021.109684.

[110] S. N, A.K. Srinivasan, K. P, J.S. S, A.K. G, Schiff's base (SB) modified zirconium dioxide reinforced PLA bio-composite film for industrial packaging applications, Composites Communications 25 (2021) 100750, https://doi.org/https://doi.org/10.1016/j.coco.2021.100750.

[111] X.G. Wang, S.H. Wang, W.J. Wang, H.F. Li, X.D. Liu, X.Y. Gu, S. Bourbigot, Z.W. Wang, J. Sun, S. Zhang, The flammability and mechanical properties of poly (lactic acid) composites containing Ni-MOF nanosheets with polyhydroxy groups, Compos Part B-Eng 183 (2020) 107568, https://doi.org/10.1016/j.compositesb.2019.107568.

[112] Lu Zhang, Siqi Chen, Ye-Tang Pan, Shuidong Zhang, Shibin Nie, Ping Wei, Xiuqin Zhang, Rui Wang, and De-Yi Wang,Nickel Metal–Organic Framework Derived Hierarchically Mesoporous Nickel Phosphate toward Smoke Suppression and Mechanical Enhancement of Intumescent Flame Retardant Wood Fiber/Poly(lactic acid) Composites, ACS Sustain Chem Eng 7(10) (2019) 9272-9280, https://doi.org/10.1021/acssuschemeng.9b00174.

[113] M. Zhang, Y. Gao, Y. Zhan, X. Ding, M. Wang, X. Wang, Preparing the Degradable, Flame-Retardant and Low Dielectric Constant Nanocomposites for Flexible and Miniaturized Electronics with Poly(lactic acid), Nano ZIF-8@GO and Resorcinol Di(phenyl phosphate), Materials (Basel) 11(9) (2018) 1756, https://doi.org/10.3390/ma11091756.

[114] M. Zhang, X. Ding, Y. Zhan, Y. Wang, X. Wang, Improving the flame retardancy of poly(lactic acid) using an efficient ternary hybrid flame retardant by dual modification of graphene oxide with phenylphosphinic acid and nano MOFs, J Hazard Mater 384 (2020) 121260, https://doi.org/10.1016/j.jhazmat.2019.121260.

[115] Y. Li, B. Xue, S. Wang, J. Sun, H. Li, X. Gu, H. Wang, S. Zhang, Photoaging and Fire Performance of Polypropylene Containing Melamine Phosphate, ACS Appl Polym Mater 2(11) (2020) 4455-4463, https://doi.org/10.1021/acsapm.0c00578.

[116] Y. Zhang, H. Yan, G. Feng, R. Liu, K. Yang, W. Feng, S. Zhang, C. He, Non-aromatic Si, P, N-containing hyperbranched flame retardant on reducing fire hazards of epoxy resin with desirable mechanical properties and lower curing temperature, Compos Part B-Eng 222 (2021) 109043, https://doi.org/10.1016/j.compositesb.2021.109043.

[117] W. Zhu, S. Hao, M. Yang, B. Cheng, J. Zhang, A synergistic flame retardant of glycosyl cross-linking boron acid and ammonium salt of phytic acid to enhance durable flame retardancy of cotton fabrics, Cellulose 27(16) (2020) 9699-9710, https://doi.org/10.1007/s10570-020-03417-x.

[118] X. Wang, J. Sun, X. Liu, S. Jiang, J. Wang, H. Li, S. Bourbigot, X. Gu, S. Zhang, An effective flame retardant containing hypophosphorous acid for poly (lactic acid): Fire performance, thermal stability and mechanical properties, Polym Test 78 (2019) 105940, https://doi.org/10.1016/j.polymertesting.2019.105940.

[119] B. Tawiah, B. Yu, R. Wei, R.K.K. Yuen, W. Chen, J.H. Xin, B. Fei, Simultaneous fire safety enhancement and mechanical reinforcement of poly(lactic acid) biocomposites with hexaphenyl (nitrilotris(ethane-2,1-diyl))tris(phosphoramidate), J Hazard Mater 380 (2019) 120856, https://doi.org/10.1016/j.jhazmat.2019.120856.

[120] L. Liu, Y. Xu, Y. Di, M. Xu, Y. Pan, B. Li, Simultaneously enhancing the fire retardancy and crystallization rate of biodegradable polylactic acid with piperazine-1,4-diylbis(diphenylphosphine oxide), Compos Part B-Eng 202 (2020) 108407, https://doi.org/10.1016/j.compositesb.2020.108407.

[121] L. Liu, Y. Xu, Y. Pan, M. Xu, Y. Di, B. Li, Facile synthesis of an efficient phosphonamide flame retardant for simultaneous enhancement of fire safety and crystallization rate of poly (lactic acid), Chem. Eng. J. 421 (2021) 127761, https://doi.org/10.1016/j.cej.2020.127761.

[122] P. Zhao, Z. Liu, X. Wang, Y.-T. Pan, I. Kuehnert, M. Gehde, D.-Y. Wang, A. Leuteritz, Renewable vanillin based flame retardant for poly(lactic acid): a way to enhance flame retardancy and toughness simultaneously, RSC Advances 8(73) (2018) 42189-42199, https://doi.org/10.1039/c8ra08531e.

[123] B. Tawiah, B. Yu, A.C.Y. Yuen, R.K.K. Yuen, J.H. Xin, B. Fei, Thermal, crystalline and mechanical properties of flame retarded Poly(lactic acid) with a PBO-like small molecule -

Phenylphosphonic Bis(2-aminobenzothiazole), Polym. Degrad. Stab. 163 (2019) 76-86, https://doi.org/10.1016/j.polymdegradstab.2019.03.002.

[124] J. Sun, L. Li, J. Li, Effects of furan-phosphamide derivative on flame retardancy and crystallization behaviors of poly(lactic acid), Chem. Eng. J. 369 (2019) 150-160, https://doi.org/10.1016/j.cej.2019.03.036.

[125] G. Ye, S. Huo, C. Wang, Q. Shi, Z. Liu, H. Wang, One-step and green synthesis of a bio-based high-efficiency flame retardant for poly (lactic acid), Polym. Degrad. Stab. 192 (2021) 109696, https://doi.org/10.1016/j.polymdegradstab.2021.109696.

[126] L. Long, Q. Chang, W. He, Y. Xiang, S. Qin, J. Yin, J. Yu, Effects of bridged DOPO derivatives on the thermal stability and flame retardant properties of poly(lactic acid), Polym. Degrad. Stab. 139 (2017) 55-66, https://doi.org/10.1016/j.polymdegradstab.2017.03.016.

[127] M. Niu, Z. Zhang, Z. Wei, W. Wang, Effect of a Novel Flame Retardant on the Mechanical, Thermal and Combustion Properties of Poly(Lactic Acid), Polymers (Basel) 12(10) (2020) 2407, https://doi.org/10.3390/polym12102407.

[128] Y. Bing, C. Yinghong, Z. Mingdan, Y. Gaowei, Synergistic and compatibilizing effect of octavinyl polyhedral oligomeric silsesquioxane nanoparticles in polypropylene intumescent flame retardant composite system, Compos Part A-Appl S 123 (2019) 46-58, https://doi.org/10.1016/j.compositesa.2019.04.032.

[129] L. Jia, B. Tong, D. Li, W. Zhang, R. Yang, Crystallization and flame-retardant properties of polylactic acid composites with polyhedral octaphenyl silsesquioxane, Polym Advan Technol 30(3) (2018) 648-665, https://doi.org/10.1002/pat.4501.

[130] Y. Xue, J. Feng, S. Huo, P. Song, B. Yu, L. Liu, H. Wang, Polyphosphoramide-intercalated MXene for simultaneously enhancing thermal stability, flame retardancy and mechanical properties of polylactide, Chemical Engineering Journal 397 (2020) 125336, https://doi.org/https://doi.org/10.1016/j.cej.2020.125336.

[131] Q. Ma, J. Lu, J. Yao, J. Yin, R. Zhang, F. Luo, The synergistic role of acidic molecular sieve on flame retardant performance in PLA/MF@APP composite, J Polym Res 29(5) (2022) 192, https://doi.org/10.1007/s10965-022-03037-y.

[132] N. Wu, G. Fu, Y. Yang, M. Xia, H. Yun, Q. Wang, Fire safety enhancement of a highly efficient flame retardant poly(phenylphosphoryl phenylenediamine) in biodegradable poly(lactic acid), Journal of Hazardous Materials 363 (2019) 1-9, https://doi.org/https://doi.org/10.1016/j.jhazmat.2018.08.090.

[133] Y. Xue, M. Shen, Y. Zheng, W. Tao, Y. Han, W. Li, P. Song, H. Wang, One-pot scalable fabrication of an oligomeric phosphoramide towards high-performance flame retardant polylactic acid with a submicron-grained structure, Compos Part B-Eng 183 (2020) 107695, https://doi.org/10.1016/j.compositesb.2019.107695.

[134] Y. Xue, Z. Ma, X. Xu, M. Shen, G. Huang, S. Bourbigot, X. Liu, P. Song, Mechanically robust and flame-retardant polylactide composites based on molecularly-engineered polyphosphoramides, Compos Part A-Appl S 144 (2021) 106317, https://doi.org/10.1016/j.compositesa.2021.106317.

[135] S. Zhou, Y. Yang, Z. Zhu, Z. Xie, X. Sun, C. Jia, F. Liu, J. Wang, J. Yang, Preparation of a halogen-free flame retardant and its effect on the poly(L-lactic acid) as the flame retardant material, Polymer 229 (2021) 124027, https://doi.org/10.1016/j.polymer.2021.124027.

[136] G. Liu, S. Gao, Synergistic effect between aluminum hypophosphite and a new intumescent flame retardant system in poly(lactic acid), J Appl Polym Sci 135(23) (2018) 46359, https://doi.org/10.1002/app.46359.

[137] J. Feng, X. Xu, Z. Xu, H. Xie, P. Song, L. Li, G. Huang, H. Wang, One-Pot, Solvent- and Catalyst-Free Synthesis of Polyphosphoramide as an Eco-Benign and Effective Flame Retardant for Poly(lactic acid), ACS Sustain. Chem. Eng 8(44) (2020) 16612-16623, https://doi.org/10.1021/acssuschemeng.0c05931.

[138] J. Feng, Z. Ma, Z. Xu, H. Xie, Y. Lu, C. Maluk, P. Song, S. Bourbigot, H. Wang, A Si-containing polyphosphoramide via green chemistry for fire-retardant polylactide with well-preserved mechanical and transparent properties, Chem. Eng. J. 431 (2022) 134259, https://doi.org/10.1016/j.cej.2021.134259.

[139] T. Liu, J. Jing, Y. Zhang, Z. Fang, Synthesis of a novel polyphosphate and its application with APP in flame retardant PLA, RSC Advances 8(8) (2018) 4483-4493, https://doi.org/10.1039/c7ra12582h.

[140] X.-W. Cheng, J.-P. Guan, X.-H. Yang, R.-C. Tang, F. Yao, A bio-resourced phytic acid/chitosan polyelectrolyte complex for the flame retardant treatment of wool fabric, J Clean Prod 223 (2019) 342-349, https://doi.org/10.1016/j.jclepro.2019.03.157.

[141] C. Kumar Kundu, W. Wang, S. Zhou, X. Wang, H. Sheng, Y. Pan, L. Song, Y. Hu, A green approach to constructing multilayered nanocoating for flame retardant treatment of polyamide 66 fabric from chitosan and sodium alginate, Carbohydr Polym 166 (2017) 131-138, https://doi.org/10.1016/j.carbpol.2017.02.084.

[142] Y. Zhou, B. Tawiah, N. Noor, Z. Zhang, J. Sun, R.K.K. Yuen, B. Fei, A facile and sustainable approach for simultaneously flame retarded, UV protective and reinforced poly(lactic acid) composites using fully bio-based complexing couples, Compos Part B-Eng 215 (2021) 108833, https://doi.org/10.1016/j.compositesb.2021.108833.

[143] Y. Li, S. Qiu, J. Sun, Y. Ren, S. Wang, X. Wang, W. Wang, H. Li, B. Fei, X. Gu, Sheng Zhang, A new strategy to prepare fully bio-based poly(lactic acid) composite with high flame retardancy, UV resistance, and rapid degradation in soil, Chem. Eng. J. 428 (2022) 1385-8947, https://doi.org/10.1016/j.cej.2021.131979.

[144] D. Xiao, J.X. Lv, F.J. Wu, Z.B. Wang, K. Harre, J.H. Chen, U. Gohs, D.Y. Wang, Development of multifunctional highly-efficient bio-based fire-retardant poly(lactic acid) composites for simultaneously improving thermal, crystallization and fire safety properties, Int J Biol Macromol. 215(31) (2022) 646-656, https://doi.org/10.1016/j.ijbiomac.2022.06.158.

[145] F. Kong, Q. He, W. Peng, S. Nie, X. Dong, J. Yang, Eco-friendly flame retardant poly(lactic acid) composites based on banana peel powders and phytic acid: flame retardancy and thermal property, J Polym Res 27(204) (2020) 1-12, https://doi.org/10.1007/s10965-020-02176-4.

[146] B. Tawiah, B. Yu, S. Ullah, R. Wei, R.K.K. Yuen, J.H. Xin, B. Fei, Flame retardant poly(lactic acid) biocomposites reinforced by recycled wool fibers – Thermal and mechanical properties, Express Polym Lett 13(8) (2019) 697-712, https://doi.org/10.3144/expresspolymlett.2019.59.

[147] Y. Yang, L. Haurie, J. Wen, S. Zhang, A. Ollivier, D.-Y. Wang, Effect of oxidized wood flour as functional filler on the mechanical, thermal and flame-retardant properties of polylactide biocomposites, Ind Crop Prod 130 (2019) 301-309, https://doi.org/10.1016/j.indcrop.2018.12.090.

[148] T. Yu, T. Tuerhongjiang, C. Sheng, Y. Li, Phosphorus-containing diacid and its application in jute/poly(lactic acid) composites: Mechanical, thermal and flammability properties, Compos Part A-Appl S 97 (2017) 60-66, https://doi.org/10.1016/j.compositesa.2017.03.004.

[149] S. Hazer, M. Coban, A. Aytac, Effects of ammonium polyphosphate and triphenyl phosphate on the flame retardancy, thermal, and mechanical properties of glass fiber-reinforced PLA/PC composites, Fire Mater 43(3) (2019) 277-282, https://doi.org/10.1002/fam.2696.

[150] J. Zhan, J. Wang, J. Lin, G. Zhao, S. Ji, X. Li, J. Li, G. Wang, L. Chen, Y. Guan, H. Naceur, Flame-retardant, thermal and mechanical properties of PLA/ramie fiber composites, Polym Composite 43(7) (2022) 4244-4254, https://doi.org/10.1002/pc.26685.

[151] G. Sanchez-Olivares, A. Sanchez-Solis, F. Calderas, J. Alongi, Keratin fibres derived from tannery industry wastes for flame retarded PLA composites, Polymer Degradation and Stability 140 (2017) 42-54, https://doi.org/https://doi.org/10.1016/j.polymdegradstab.2017.04.011.

[152] L. Hu, Z. Fu, X. Gu, H. Wang, Y. Li, Strengthened interface as flame retarding belt: Compatibilized PLLA/PP blends by reactive boehmite nanorods, Polymer 228 (2021) 123879, https://doi.org/10.1016/j.polymer.2021.123879.

[153] Y. Zhou, S. Qiu, G.I.N. Waterhouse, K. Zhang, J. Xu, Enhancing the properties of PBAT/PLA composites with novel phosphorus-based ionic liquid compatibilizers, Mater Today Commun 27 (2021) 102407, https://doi.org/10.1016/j.mtcomm.2021.102407.

[154] S. Li, L. Deng, C. Xu, Q. Wu, Z. Wang, Making a Supertough Flame-Retardant Polylactide Composite through Reactive Blending with Ethylene-Acrylic Ester-Glycidyl Methacrylate Terpolymer and Addition of Aluminum Hypophosphite, ACS Omega 2(5) (2017) 1886-1895, https://doi.org/10.1021/acsomega.7b00162.

[155] T. Suparanon, N. Phusunti, W. Phetwarotai, Properties and characteristics of polylactide blends: Synergistic combination of poly(butylene succinate) and flame retardant, Polym Advan Technol 29(2) (2018) 785-794, https://doi.org/10.1002/pat.4184.

[156] Y. Sun, S. Sun, L. Chen, L. Liu, P. Song, W. Li, Y. Yu, L. Fengzhu, J. Qian, H. Wang, Flame retardant and mechanically tough poly(lactic acid) biocomposites via combining ammonia polyphosphate and polyethylene glycol, Compos. Commun. 6 (2017) 1-5, https://doi.org/10.1016/j.coco.2017.07.005.

[157] N. Wu, J. Yu, W. Lang, X. Ma, Y. Yang, Flame Retardancy and Toughness of Poly(Lactic Acid)/GNR/SiAHP Composites, Polymers (Basel) 11(7) (2019) 1129, https://doi.org/10.3390/polym11071129.

[158] D.-F. Li, X. Zhao, Y.-W. Jia, L. He, X.-L. Wang, Y.-Z. Wang, Dual effect of dynamic vulcanization of biobased unsaturated polyester: Simultaneously enhance the toughness and fire safety of Poly(lactic acid), Compos Part B-Eng 175 (2019) 107069, https://doi.org/10.1016/j.compositesb.2019.107069.

[159] D.-F. Li, X. Zhao, Y.-W. Jia, L. He, X.-L. Wang, Y.-Z. Wang, Simultaneously enhance both the flame retardancy and toughness of polylactic acid by the cooperation of intumescent flame retardant and bio-based unsaturated polyester, Polym. Degrad. Stab. 168 (2019) 108961, https://doi.org/10.1016/j.polymdegradstab.2019.108961.

[160] J. Harada, A.G. de Souza, J.R.N. de Macedo, D.S. Rosa, Soil culture: Influence of different natural fillers incorporated in biodegradable mulching film, J Mol Liq 273 (2019) 33-36, https://doi.org/10.1016/j.molliq.2018.09.109.

[161] X. Li, S. Gong, L. Yang, X. Xia, C. Linghu, J. Wang, Z. Luo, Transesterification catalyzed via ferric chloride for fabricating Poly(lactic acid)/Poly(butylene adipate-co-terephthalate) blends with ultra-fast degradation and high toughness, Polymer 228 (2021) 123927, https://doi.org/10.1016/j.polymer.2021.123927.

[162] J. Zhao, H. Pan, H. Yang, J. Bian, H. Zhang, G. Gao, L. Dong, Study on miscibility, thermal properties, degradation behaviors, and toughening mechanism of poly(lactic acid)/poly (ethylene-butylacrylate-glycidyl methacrylate) blends, Int J Biol Macromol 143 (2020) 443-452, https://doi.org/10.1016/j.ijbiomac.2019.11.226.

[163] M.L. Iglesias-Montes, M. Soccio, V. Siracusa, M. Gazzano, N. Lotti, V.P. Cyras, L.B. Manfredi, Chitin Nanocomposite Based on Plasticized Poly(lactic acid)/Poly(3-hydroxybutyrate) (PLA/PHB) Blends as Fully Biodegradable Packaging Materials, Polymers 14(15) (2022) 3177, https://doi.org/10.3390/polym14153177.

[164] M. Ma, X. Wang, K. Liu, S. Chen, Y. Shi, H. He, X. Wang, Simultaneously enhanced fracture toughness and flame-retardant property of poly(l-lactic acid) via reactive blending with ammonium polyphosphate and in situ formed polyurethane, Polym Int 69(10) (2020) 985-994, https://doi.org/10.1002/pi.6053.

[165] D.-F. Li, X. Zhao, Y.-W. Jia, X.-L. Wang, Y.-Z. Wang, Tough and flame-retardant poly(lactic acid) composites prepared via reactive blending with biobased ammonium phytate and in situ formed crosslinked polyurethane, Compos. Commun. 8 (2018) 52-57, https://doi.org/10.1016/j.coco.2018.04.001.

[166] W. Phetwarotai, T. Suparanon, N. Phusunti, P. Potiyaraj, Influence of compatibilizer and multifunctional additive loadings on flame retardation, plasticization, and impact modification of polylactide and poly(butylene adipate-co-terephthalate) biodegradable blends, Polym Advan Technol 31(9) (2020) 2094-2107, https://doi.org/10.1002/pat.4932.

[167] S. Yu, H. Xiang, J. Zhou, M. Zhu, Enhanced flame-retardant performance of poly (lactic acid) (PLA) composite by using intrinsically phosphorus-containing PLA, Prog Nat Sci-Mater 28(5) (2018) 590-597, https://doi.org/10.1016/j.pnsc.2018.09.002.

[168] R. Mincheva, H. Guemiza, C. Hidan, S. Moins, O. Coulembier, P. Dubois, F. Laoutid, Development of Inherently Flame-Retardant Phosphorylated PLA by Combination of Ring-Opening Polymerization and Reactive Extrusion, Materials (Basel) 13(1) (2019) 13, https://doi.org/10.3390/ma13010013.

[169] W. Hu, Y. Zhang, Y. Qi, H. Wang, B. Liu, Q. Zhao, J. Zhang, J. Duan, L. Zhang, Z. Sun, B. Liu, Improved Mechanical Properties and Flame Retardancy of Wood/PLA All-Degradable Biocomposites with Novel Lignin-Based Flame Retardant and TGIC, Macromolecular Materials and Engineering 305(5) (2020) 1900840, https://doi.org/https://doi.org/10.1002/mame.201900840.

[170] X. Hu, J. Sun, X. Li, L. Qian, J. Li, Effect of phosphorus–nitrogen compound on flame retardancy and mechanical properties of polylactic acid, J Appl Polym Sci 138(7) (2020) 49829, https://doi.org/10.1002/app.49829.

[171] J. Zhan, G. Wang, J. Li, Y. Guan, G. Zhao, H. Naceur, D. Coutellier, J. Lin, Effect of the compatilizer and chemical treatments on the performance of poly(lactic acid)/ramie fiber composites, Compos. Commun. 27 (2021) 100843, https://doi.org/10.1016/j.coco.2021.100843.

[172] H. Wu, M. Hao, Strengthening and Toughening of Polylactide/Sisal Fiber Biocomposites via in-situ Reaction with Epoxy-Functionalized Oligomer and Poly (butylene-adipate-terephthalate), Polymers (Basel) 11(11) (2019) 1747, https://doi.org/10.3390/polym11111747.

[173] B.W. Liu, H.B. Zhao, Y.Z. Wang, Advanced Flame-Retardant Methods for Polymeric Materials, Adv Mater (2021) e2107905, https://doi.org/10.1002/adma.202107905.

[174] M.-O. Augé, D. Roncucci, S. Bourbigot, F. Bonnet, S. Gaan, G. Fontaine, Recent advances on reactive extrusion of Poly(lactic acid), Eur Polym J 184 (2023), https://doi.org/10.1016/j.eurpolymj.2022.111727.

[175] D.A. Villamil Watson, D.A. Schiraldi, Biomolecules as Flame Retardant Additives for Polymers: A Review, Polymers (Basel) 12(4) (2020), https://doi.org/10.3390/polym12040849.

[176] C. Sun, S. Wei, H. Tan, Y. Huang, Y. Zhang, Progress in upcycling polylactic acid waste as an alternative carbon source: A review, Chem. Eng. J. 446(1) (2022) 136881, https://doi.org/10.1016/j.cej.2022.136881.

[177] T. Li, H. Sun, H. Han, C. Zhang, B. Li, J. Huang, D. Sun, Ultrafast bulk degradation of polylactic acid by artificially cultured diatom frustules, Compos Sci Technol 223 (2022) 109410, https://doi.org/10.1016/j.compscitech.2022.109410.